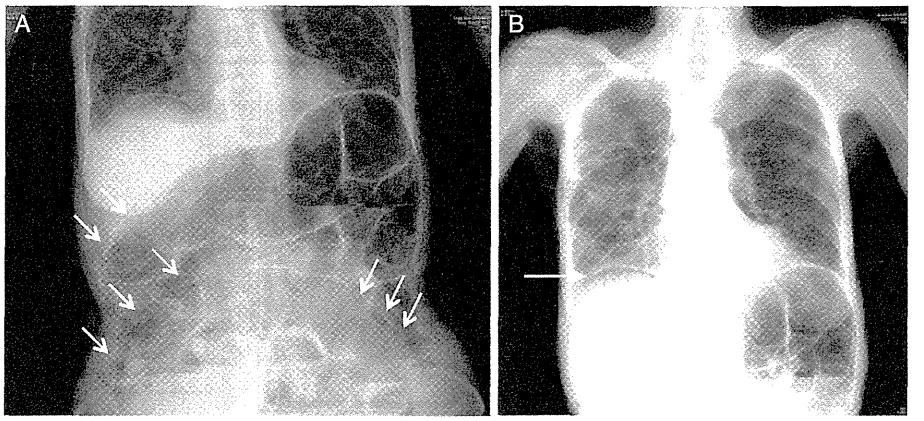

図1　単純X線検査(69歳女性，強皮症)
A：腹部X線，B：胸部X線

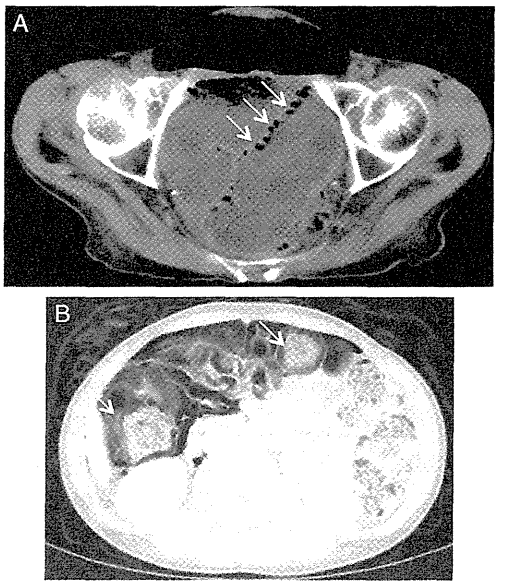

図2　腹部CT検査
A：図1と同一症例，
B:31歳女性，結節性多発動脈炎．ステロイド投与後．

し，腸管内ガスが粘膜の微細な損傷部位から腸管壁内に侵入して気腫が形成される．

2．細 菌 説

腸内細菌が粘膜下に侵入してガスを産生する．

3．化 学 説

トリクロロエチレンの慢性曝露，ステロイドやα-グルコシダーゼ阻害薬使用と関連する．

4．慢性肺疾患説

喘息，慢性気管支炎において，胸腔内圧上昇により肺胞から漏れた空気が縦隔気腫をきたし，後腹膜腔から腸管膜を介して腸管壁に侵入する．

診　断

PCIの診断は，さまざまな画像検査によって行われるが，主な手段は1と2である．

1．胸腹部単純X線検査

腹部X線では，腸管の走行に沿って，類円形で大小不同のブドウの房様の透亮像が認められる(図1-A)．腸管運動低下やガス産生を反映して大量の腸管ガスも伴う．また，胸部X線では横隔膜下にしばしば腹腔内遊離ガス像を認める(図1-B)．

2．腹部CT検査

最も感度の高い検査であり，診断のゴールドスタンダードである[4]．腸管壁内に小円形の気腫を複数認める例(図2-A)や，腸管壁全周性に気腫を認める例(図2-B)がある．また，腹腔内遊離ガス像も約70％の例でみられる[5]．一般的に，腹腔内遊離ガス像の原因はそのほとんどが消化管穿孔であるため，消化管穿孔による腹膜炎や腸管壊死との鑑別にきわめて有用なCTはPCIの診断に必須な検査である．

3．大腸内視鏡

粘膜下腫瘍様隆起が集簇して多発する．表面は平滑で弾力性があり，一部発赤を伴う(図3)．

4．注腸造影検査

平滑な隆起性病変を認める(図4)．

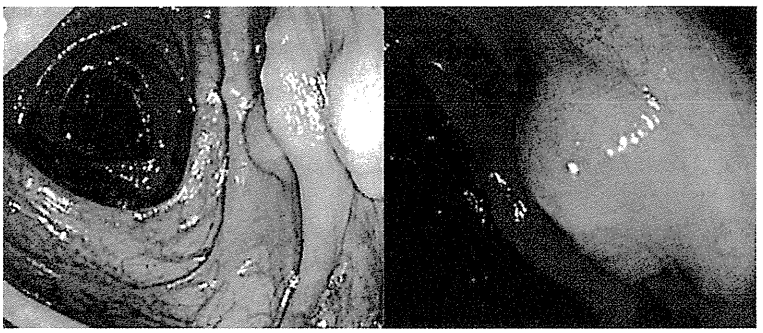

図3 大腸内視鏡検査
19歳男性，基礎疾患なし．

治　療

本症の治療法は保存的治療が原則である．禁食，中心静脈栄養（または経腸成分栄養），α-グルコシダーゼ阻害薬の内服があればその中止をまず行う．腸管内のガス貯留が多い場合は，嫌気性菌によるガス産生亢進が考えられることから，metronidazoleの有効性が報告されている[6]．Metronidazoleが使用できない場合は，ampicillin，tetracycline，vancomycinも使用される．

PCIに特徴的な治療として，酸素吸入療法があげられる．腸管壁の気腫の内容は窒素が約90%であることが報告されているが，窒素は通常環境下では組織への移行が悪い[7]．そこで，血液中の酸素分圧を上げることで，閉鎖腔の窒素が組織への吸収がよい酸素に置換され，気腫の縮小が促進される[8]．特に，高気圧下ではこの作用が増強されることから高気圧酸素療法が有効と考えられており，わが国では，2～3気圧，1～2時間，10日間程度で良好な成績が報告されている[9]．ただし，高気圧酸素療法室が使用できる施設は限られるため，代わりに高流量酸素療法も試みられている[10]．また，再発する場合は酸素療法を繰り返す．

大部分は保存的治療と酸素療法で軽快するが，腸管虚血や腸重積を合併することもあり，腹膜刺激症状，炎症反応上昇，アシドーシス（pH＜7.3），門脈血中ガスを認めた場合は外科的治療を考慮する．

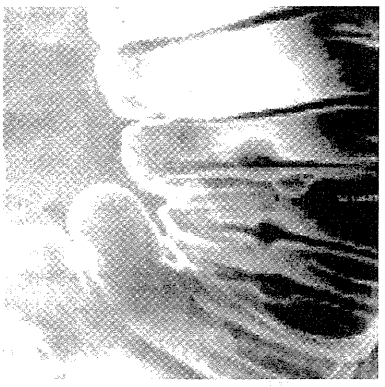

図4 注腸検査
図3と同一症例．

膠原病におけるPCI

PCIは，さまざまな膠原病での報告があり，そのなかで約半数が強皮症である[5)11)]．次いで皮膚筋炎が多い[12]．SLE[13]とMCTD[14]でも複数の報告があり，稀ではあるが多発性筋炎，結節性多発動脈炎，巨細胞性動脈炎，原発性シェーグレン症候群，再発性多発軟骨炎，ベーチェット病でも起こりえる[5)15)16)]．われわれは成人発症スチル病での発症も経験している．このことから，PCIは膠原病全般に発症しうると考えられる．

強皮症以外のPCI症例のほとんどはステロイド投与後に発症していることから，膠原病関連PCIは強皮症とステロイド治療関連の2つの発症機序に分けられる．強皮症では，固有の下部消化管病変による腸管壁運動低下とそれに伴う腸内細菌増殖，ガス過剰産生を呈する．これにより腸管内圧が上昇し，ガスが物理的に壁内に侵入して

気腫を形成すると考えられている．一方，ステロイド関連では，腸管粘膜の脆弱化やPeyer板の縮小化が生じ，腸管粘膜の透過性が亢進してガスが侵入する機序が考えられる[17]．自験例や文献に基づく私見であるが，興味深いことに，強皮症では小円形の気腫が壁内に多数みられるのに対し(図2-A)，ステロイド使用例では気腫が腸管の全周性に連続してみられる傾向があった(図2-B)．この気腫の形状の違いは，内圧亢進による機序と，組織脆弱性による機序をそれぞれ反映している可能性が考えられる．

治療は前述の内容に準じるが，ステロイド使用例では，α-グルコシダーゼ阻害薬・トリクロロエチレン使用例と異なり短期間で中止できない．したがって，保存的治療と酸素療法で慎重に経過を観察せざるをえない．また，強皮症では，モサプリド，オクトレオチドなど腸管運動促進薬も有用な場合がある[18]．われわれは，間質性肺疾患をもつ強皮症で，PCIに対して在宅酸素，在宅中心静脈栄養，腸管運動促進薬，抗生剤を導入し，摂食可能となり，中心動脈栄養を中止するまで回復した例を経験した(図1，図2-A)．膠原病関連PCIでは，基礎疾患の状態も考慮し，総合的な管理を行うことが求められる．

おわりに

PCIを疑った場合，最も重要なことはCT検査で緊急性のある消化管穿孔と鑑別を的確に行うことである．PCIであれば外科的治療は原則不要で，時間を要するが，保存的治療に酸素療法を加えることで管理できる場合が多い．個々の症例の病態に応じた全身管理を行うことが肝要である．

文　献

1) Pizzala J, Pogorelsky V, González M, et al. Pneumatosis cystoides intestinalis : a case report and review of the literature. Acta Gastroenterol Latinoam 2014 ; 44 : 48.
2) Koss LG. Abdominal gas cysts (pneumatosis cystoides intestinorum hominis) ; an analysis with a report of a case and a critical review of the literature. AMA Arch Pathol 1952 ; 53 : 523.
3) Jamart J. Pneumatosis cystoides intestinalis. A statistical study of 919 cases. Acta Hepatogastroenterol (Stuttg) 1979 ; 26 : 419.
4) Lee KS, Hwang S, Hurtado Rúa SM, et al. Distinguishing benign and life-threatening pneumatosis intestinalis in patients with cancer by CT imaging features. AJR Am J Roentgenol 2013 ; 200 : 1042.
5) Balbir-Gurman A, Brook OR, Chermesh I, Braun-Moscovici Y. Pneumatosis cystoides intestinalis in scleroderma-related conditions. Intern Med J 2012 ; 42 : 323.
6) Ellis BW. Symptomatic treatment of primary pneumatosis coli with metronidazole. Br Med J 1980 ; 280 : 763.
7) Mujahed Z, Evans JA. Gas cysts of the intestine (pneumatosis intestinalis). Surg Gynecol Obstet 1958 ; 107 : 151.
8) Forgacs P, Wright PH, Wyatt AP. Treatment of intestinal gas cysts by oxygen breathing. Lancet 1973 ; 1 : 579.
9) Shimada M, Ina K, Takahashi H, et al. Pneumatosis cystoides intestinalis treated with hyperbaric oxygen therapy : usefulness of an endoscopic ultrasonic catheter probe for diagnosis. Intern Med 2001 ; 40 : 896.
10) Holt S, Gilmour HM, Buist TA, et al. High flow oxygen therapy for pneumatosis coli. Gut 1979 ; 20 : 493.
11) Sequeira W. Pneumatosis cystoides intestinalis in systemic sclerosis and other diseases. Semin Arthritis Rheum 1990 ; 19 : 269.
12) Xiao T, Xu HH, Wu J, et al. Case of pneumatosis cystoides intestinalis in adult dermatomyositis. J Dermatol 2008 ; 35 : 49.
13) Mizoguchi F, Nanki T, Miyasaka N. Pneumatosis cystoides intestinalis following lupus enteritis and peritonitis. Intern Med 2008 ; 47 : 1267.
14) Aoki Y, Nagashima T, Kamimura T, et al. Marked pneumatosis cystoides intestinalis in a patient with mixed connective tissue disease. J Rheumatol 2006 ; 33 : 1705.
15) Dovrish Z, Arnson Y, Amital H, Zissin R. Pneumatosis intestinalis presenting in autoimmune

diseases : a report of three patients. Ann N Y Acad Sci 2009 ; 1173 : 199.
16) Grasland A, Pouchot J, Leport J, et al. Pneumatosis cystoides intestinalis in systemic diseases : 3 cases. Presse Med 1998 ; 27 : 1785.
17) Heng Y, Schuffler MD, Haggitt RC, Rohrmann CA. Pneumatosis intestinalis : a review. Am J Gastroenterol 1995 ; 90 : 1747.
18) Soudah HC, Hasler WL, Owyang C. Effect of octreotide on intestinal motility and bacterial overgrowth in scleroderma. N Engl J Med 1991 ; 325 : 1461.

* * *

EBI3 Downregulation Contributes to Type I Collagen Overexpression in Scleroderma Skin

Hideo Kudo,[1] Zhongzhi Wang,[1] Masatoshi Jinnin, Wakana Nakayama, Kuniko Inoue, Noritoshi Honda, Taiji Nakashima, Ikko Kajihara, Katsunari Makino, Takamitsu Makino, Satoshi Fukushima, and Hironobu Ihn

IL-12 family cytokines are implicated in the pathogenesis of various autoimmune diseases, but their role in the regulation of extracellular matrix expression and its contribution to the phenotype of systemic sclerosis (SSc) remain to be elucidated. Among the IL-12 family members, IL-35 decreases type I collagen expression in cultured dermal fibroblasts. IL-35 consists of p35 and EBI3 subunits, and EBI3 alone could downregulate the protein and mRNA expression of type I or type III collagen in the presence or absence of TGF-β costimulation. We found that collagen mRNA stability was reduced by EBI3 via the induction of miR-4500. The IL-35 levels in the sera or on the surface of T cells were not altered in SSc patients, while EBI3 expression was decreased in the keratinocytes of the epidermis and regulatory T cells of the dermis in SSc skin compared with normal skin, which may induce collagen synthesis in SSc dermal fibroblasts. We also found that gp130, the EBI3 receptor, was expressed in both normal and SSc fibroblasts. Moreover, we revealed that EBI3 supplementation by injection into the skin improves mice skin fibrosis. Decreased EBI3 in SSc skin may contribute to an increase in collagen accumulation and skin fibrosis. Clarifying the mechanism regulating the extracellular matrix expression by EBI3 in SSc skin may lead to better understanding of this disease and new therapeutic strategies using ointment or microinjection of the subunit. ***The Journal of Immunology*****, 2015, 195: 3565–3573.**

Systemic sclerosis (SSc) is a connective tissue disorder characterized by fibrosis of the skin and internal organs. The hallmark of this disease is the activation of fibroblasts and excessive deposition of the extracellular matrix (ECM), mainly type I collagen, which consists of α1(I) and α2(I) collagen (1, 2). The interactions among endothelial cells, lymphocytes and/or macrophages may trigger the activation of fibroblasts (3, 4), which is mediated by cytokines and growth factors, such as TGF-β1, connective tissue growth factor, platelet-derived growth factor (PDGF), insulin-like growth factor (IGF) and IL-1, IL-6, and/or IL-7 (5–12). Accordingly, investigation of the cytokine network mediating fibroblast activation of SSc will be useful for clarifying the molecular mechanism(s) of this disease.

Department of Dermatology and Plastic Surgery, Faculty of Life Sciences, Kumamoto University, Kumamoto 860-8556, Japan

[1]H.K. and Z.W. equally contributed to this work.

ORCID: 0000-0001-8920-1447 (H.K.).

Received for publication October 2, 2014. Accepted for publication August 5, 2015.

This work was supported by a grant for scientific research from the Japanese Ministry of Education, Science, Sports and Culture, by project research on intractable diseases from the Japanese Ministry of Health, Labour and Welfare, and by a scholarship from the Graduate School of Medical Sciences, Kumamoto University, Japan.

The dataset presented in this article has been submitted to the Gene Expression Omnibus (http://www.ncbi.nlm.nih.gov/geo/) under accession number GSE68649.

Address correspondence and reprint requests to Dr. Masatoshi Jinnin, Department of Dermatology and Plastic Surgery, Faculty of Life Sciences, Kumamoto University, Honjo 1-1-1, Kumamoto 860-8556, Japan. E-mail address: mjin@kumamoto-u.ac.jp

The online version of this article contains supplemental material.

Abbreviations used in this article: CAT, chloramphenicol acetyltransferase; Ct, threshold cycle; DM, dermatomyositis; EBI3, Epstein Barr virus–induced gene; ECM, extracellular matrix; IGF, insulin-like growth factor; lcSSc, limited cutaneous systemic sclerosis; miRNA, microRNA; PDGF, platelet-derived growth factor; PIPC, pro-collagen type I C-peptide; SLE, systemic lupus erythematosus; SSc, systemic sclerosis; SSD, scleroderma spectrum disorder; Treg, regulatory T cell.

www.jimmunol.org/cgi/doi/10.4049/jimmunol.1402362

The IL-12 family cytokines (IL-12, IL-23, IL-27, and IL-35) are heterodimeric proteins that share subunits, and are produced by APCs, including macrophages and dendritic cells. Although they play roles in the regulation of T cell differentiation, the effect of each cytokine may be different; for example, IL-12 and IL-27 regulate Th1 differentiation, while IL-23 is essential for Th17 survival.

In the current study, we investigated the effects of IL-12 family cytokines on ECM expression. We found that IL-35 and its EBI3 subunit downregulate the expression of collagen. In addition, we also compared the expression pattern of IL-35 and EBI3 in the sera and skin between normal subjects and SSc patients, and demonstrated the involvement of EBI3 signaling in the abnormal ECM regulation seen in SSc.

Materials and Methods

Reagents

Recombinant human IL-12, IL-23, IL-27 and TGF-β were obtained from R&D systems (Minneapolis, MN). Human IL-35 was purchased from Chimerigen Laboratories (San Diego, CA). Human p19 and p28 were obtained from Abnova (Taipei, Taiwan). Human p35, p40, Epstein Barr virus–induced gene 3 (EBI3) and mouse EBI3 were from PROSPEC (Ness Ziona, Israel).

Patients

Serum samples were obtained from 33 patients with SSc (5 males and 28 females; age range, 24–85 y; mean, 58.7 y): 13 patients had diffuse cutaneous SSc and 20 had limited cutaneous SSc (lcSSc). All patients fulfilled the criteria the proposed by the American College of Rheumatology (13). Ten patients with systemic lupus erythematosus (SLE), 12 patients with dermatomyositis (DM) and 9 patients with scleroderma spectrum disorder (SSD), who did not fulfill the American College of Rheumatology criteria for SSc but were likely to develop SSc in the future based on proposed criteria (14–16), were also included. Control serum samples were collected from 15 healthy volunteers. PBMCs were obtained from heparinized venous blood of SSc patents, SLE patients and healthy volunteers using gradient centrifugation over Vacutainer CPT (BD, Franklin Lakes, NJ) (17, 18). The skin biopsy specimens from SSc patients were obtained from lesional skin. Control skin samples were from routinely discarded skin of healthy human subjects undergoing skin grafts.

Institutional review board approval and written informed consent were obtained before the patients and healthy volunteers were entered into this study, according to the Declaration of Helsinki.

Cell cultures

Human dermal fibroblasts were obtained by skin biopsies from normal skin of 7 healthy human subjects and affected dorsal forearm of 7 diffuse cutaneous SSc patients (19). Institutional Review Board approval and written informed consent were obtained according to the Declaration of Helsinki. Monolayer cultures independently isolated from different individuals were maintained at 37°C in 5% CO_2 in air. The cells were serum-starved for 24 h before all experiments.

Cell lysis and immunoblotting

Cultured fibroblasts were washed twice with cold PBS and lysed in Denaturing Cell Extraction Buffer (Biosource International, Camarillo, CA). Aliquots of the cell lysates (normalized for the protein concentrations) were separated by electrophoresis on 10% $NaDodSO_4$-polyacrylamide gels and transferred onto polyvinylidene difluoride filters. The polyvinylidene difluoride filters were then incubated with Abs against type I collagen (Southern Biotech, Birmingham, AL), gp130 or β-actin (Santa Cruz Biotechnology, Santa Cruz, CA). The filters were incubated with the appropriate secondary Ab, and the immunoreactive bands were visualized using ECL system (Amersham Biosciences, Arlington Heights, IL).

The measurement of Procollagen Type I

The concentration of procollagen type I was measured using the Procollagen Type I C-peptide (PIPC) EIA Kit (Takara Bio, Shiga, Japan) according to the manufacturer's instructions (20). Briefly, primary Ab against pro-collagen type I C-peptide (PIPC) was precoated onto microtitration plates. Samples were added into each well, followed by incubation with a peroxidase-labeled anti-PIPC secondary Ab. The absorbance of the solution was measured at 450 nm using a microplate reader. The concentration of PICP in the samples was calculated from the standard curve.

RNA isolation, array analysis and quantitative real-time PCR

Total RNA was extracted from cultured cells with ISOGEN (Nippon Gene, Tokyo, Japan) or from paraffin-embedded sections with RNeasy FFPE kit (Qiagen, Valencia, CA).

For the array, first-strand cDNA was synthesized from the RNA using RT^2 First Strand Kit (Qiagen). The cDNA was mixed with RT^2 SYBR Green/Rox qPCR Master Mix (Qiagen), and the mixture was added to 96-well Extracellular Matrix and Adhesion Molecules PCR Array (Qiagen). PCR was performed on Takara Thermal Cycler Dice (TP800) (Takara Bio, Shiga, Japan). The threshold cycle (Ct) for each gene was determined using Thermal Cycler Dice Real Time System version 2.10B (Takara Bio). The raw Ct was normalized using the values of housekeeping genes.

For quantitative real-time PCR, first-strand cDNA was synthesized using the PrimeScript RT reagent Kit (Takara Bio) (21). The GAPDH primer was purchased from Qiagen, and the other primers were from Takara Bio. DNA was amplified for 40 cycles of denaturation for 5 s at 95°C and annealing for 30 s at 60°C, on Takara Thermal Cycler Dice. The relative expression of each gene of interest and GAPDH were calculated by the standard curve method.

microRNAs (miRNAs) were obtained from the total RNA of cultured cells using RT^2 Quantitative PCR-Grade miRNA Isolation Kit (Qiagen). Mir-X miRNA First-Strand Synthesis Kit (Clontech Laboratories, Mountain View, CA) was used for cDNA synthesis from miRNAs. Primers (Takara Bio) and templates were mixed with SYBR Advantage Quantitative PCR Premix (Clontech Laboratories). DNA was amplified for 40 cycles of denaturation for 5 s at 95°C and annealing for 20 s at 60°C on TP800. The raw Ct of each miRNA was normalized to that of U6.

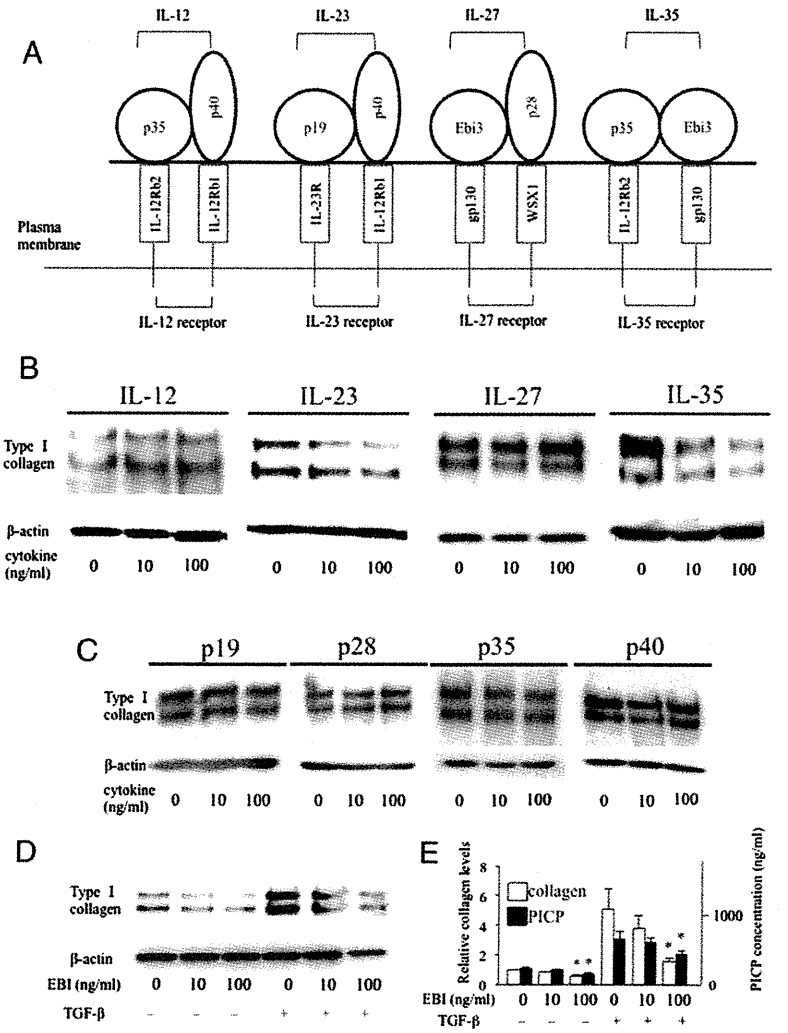

FIGURE 1. The effects of IL-12 family cytokines on the collagen expression in normal dermal fibroblasts. (**A**) The IL-12 family cytokines are composed of the α-chain (p19, p28 or p35) and β-chain (p40 or EBI3). p40 combines with p35 or p19 to form IL-12 or IL-23, respectively, while EBI3 pairs with p28 or p35 to form IL-27 or IL-35, respectively. IL-35 signals via gp130 and the IL-12 receptor β2 (IL-12Rb2). (**B**) Normal human dermal fibroblasts were serum-starved for 24 h, then were treated with IL-12 family cytokines (0–100 ng/ml) for an additional 24 h. Cell lysates were subjected to immunoblotting with an Ab against type I collagen. β-actin was used as a loading control. The results of one experiment representative of 3 independent experiments are shown. (**C**) Normal human dermal fibroblasts were treated with each subunit of the IL-12 family cytokines (0–100 ng/ml) for 24 h. Immunoblotting was performed as described in Fig.1B. The results of one experiment representative of 3 independent experiments are shown. (**D** and **E**) Normal human dermal fibroblasts were treated with EBI3 (0–100 ng/ml) for 24 h in the absence or presence of TGF-β. Immunoblotting was performed as described in Fig.1B. The result of one experiment representative of 3 independent experiments is shown (D). The protein levels of type I collagen quantitated by scanning densitometry and corrected for β-actin levels in the same samples are shown relative to the level in untreated cells (1.0, white bars). PICP levels determined as described in *Materials and Methods* are also shown (black bars). The data are expressed as the means ± SE of 3 independent experiments. $*p < 0.05$ as compared with the values in cells without EBI treatment (E).

Plasmid construction

A construct consisting of the full-length human α2(I) collagen promoter linked to the chloramphenicol acetyltransferase (CAT) reporter gene and a series of 5′-deletion of the construct were generated as described previously (22).

Transient transfection

For the CAT assay, fibroblasts were transfected with promoter constructs employing Lipofectamine 2000 (Invitrogen, Carlsbad, CA), as described previously (22). To correct for minor variations in the transfection efficiency, we included pSV-β-galactosidase vector (Promega, Madison, WI) in all transfections.

For reverse transfection, control or miR-4500 mimic (5nmol/L) mixed with Lipofectamine RNAiMAX (Invitrogen) were added when cells were plated, followed by incubation at 37°C in 5% CO_2.

CAT assay

Constructs with CAT reporter were transfected, and cells were harvested after 48 h of incubation. The CAT activities in cell lysates were assayed colorimetrically using CAT-ELISA (Roche, Mannheim, Germany) (23).

The measurement of serum IL-35 concentrations

The serum IL-35 levels were measured with the Human IL-35 ELISA Kit (Cusabio, Wuhan, China) (24). Briefly, an Ab against IL-35 was precoated onto microtiter wells. Aliquots of serum were added to each well, followed by incubation with peroxidase-conjugated Abs against IL-35. Color was developed with hydrogen peroxide and tetramethylbenzidine peroxidase, and the absorbance at 450 nm was measured. Wavelength correction was performed for absorbance at 540 nm. The concentration of IL-35 in each sample was determined by interpolation from a standard curve.

Flow cytometry

The Fc receptor of PBMCs was blocked with FcR Blocking Reagent (Miltenyi Biotec GmbH, Bergisch Gladbach, Germany). For dual color flow cytometry, the cells in each test tube were incubated for staining with a rabbit anti-CD3 Ab (Abcam, Cambridge, United Kingdom) and mouse anti-EBI3 (Abnova) or p35 (R&D) Ab. Then, the cells were incubated with an anti mouse IgG (H+L) secondary Ab, Oregon Green 488 conjugate (Thermo, Rockford, IL) and anti-rabbit PE Ab (Jackson ImmunoResearch, Suffolk, UK). Data were acquired using the Guava easyCyte flow cytometer (Millipore, Billerica, MA) to measure the fluorescence signals. $CD3^+EBI3^+$ or $CD3^+p35^+$ cells were gated based on the forward-sideward scatter profiles.

Immunohistochemistry

Wax-embedded sections (4-μm thickness) were dewaxed in xylene and rehydrated in graded alcohol. For the immunostaining of EBI3 or gp130, Ags were retrieved by incubation with citrate buffer (pH 6) for 9 min using a microwave. The endogenous peroxidase activity was inhibited with a solution of 0.3% hydrogen peroxide in methyl alcohol, after which the sections were blocked with 5% donkey serum for 20 min and then reacted

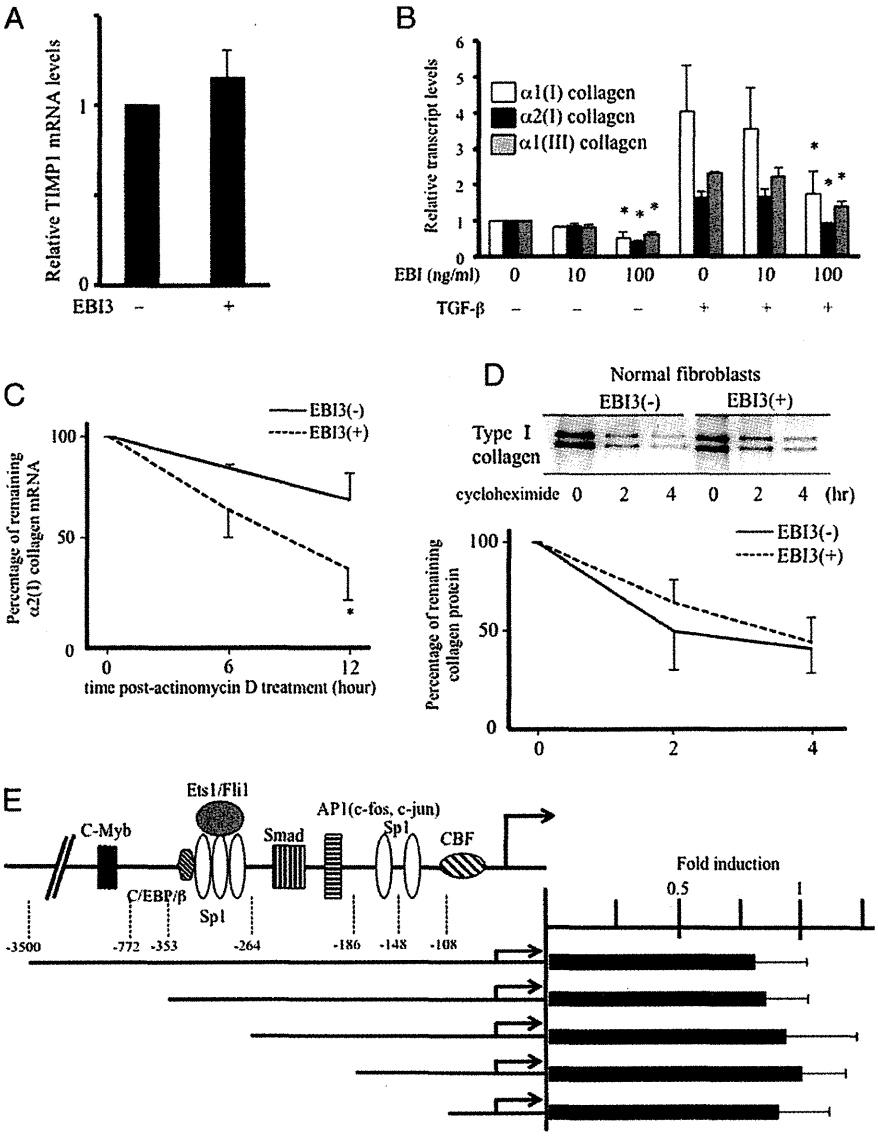

FIGURE 2. The effects of EBI3 on the type I collagen expression in normal dermal fibroblasts. **(A)** Normal human fibroblasts were treated with EBI3 (100 ng/ml) for 12 h. The mRNA levels of TIMP-1 were determined by real-time PCR (n = 3). **(B)** Normal fibroblasts were treated with EBI3 (0–100 ng/ml) for 12 h in the absence or presence of TGF-β. The mRNA levels of indicated genes were determined by real-time PCR (n = 3). *$p < 0.05$. **(C)** Fibroblasts were incubated in the presence or absence of EBI3 for 12 h before the addition with 2.5 μg/ml actinomycin D for 6 or 12 h. The α2(I) collagen mRNA expression was analyzed by real-time PCR (n = 3). The values were expressed as a percentage of the value at time 0 and are plotted on a scale. *$p < 0.05$. **(D)** *Upper panel*, Fibroblasts were incubated in the presence or absence of EBI3 for 24 h before the addition of cycloheximide (10 μg/ml). Cells were harvested at 2 or 4 h after cycloheximide was added, and immunoblotting was performed. A representative result of three independent experiments is shown. *Lower panel*, The levels of type I collagen quantitated by scanning densitometry were expressed as the percentages of the values at time 0, and were plotted on a scale (n = 3). The dotted line indicates the levels in EBI3-stimulated fibroblasts, and the solid line indicates the control levels. **(E)** The indicated α2(I) collagen promoter deletion constructs were transfected into normal fibroblasts in the absence or presence of EBI3 (100 ng/ml) for 24 h (n = 3). The bar graph represents the fold-stimulation of CAT activity in EBI3-stimulated cells relative to that in control cells (1.0).

with an Ab against EBI3 (Abcam) or gp130 (Santa Cruz Biotechnology) at 4°C. After excess Ab was washed out with PBS, the samples were incubated with HRP-labeled anti-mouse Ab (Nichirei, Tokyo, Japan) at 37°C.

The reaction was visualized using diaminobenzidine substrate system (Dojin, Kumamoto, Japan). Slides were counterstained with Mayer's hematoxylin and examined under a light microscope (Olympus BX50; Olympus, Tokyo, Japan).

Immunofluorescence

Paraffin sections were deparaffinized in xylene and rehydrated in a graded ethanol series (25). Ags were retrieved by incubation with 0.1% trypsin at 37°C for 5 min. The slides were permeabilized in 0.5% Triton-PBS for 5 min and blocked in 5% nonfat dry milk for 30 min at room temperature. As the primary Abs, rabbit anti-EBI3 (1:50; Abcam) with mouse anti-CD25 (1:20; R&D) diluted in 5% milk in PBS, were applied to the sections. The sections were incubated overnight at 4°C followed by PBS-0.05% Triton X-100 washes. Then, Alexa Fluor 488 anti-mouse and Alexa Fluor 594 anti-rabbit secondary Ab were applied to the sections. After incubation for 1 h at room temperature, the sections were washed and mounted. A Zeiss Axioskop 2 microscope (Carl Zeiss, Oberkochen, Germany) was used for detection of the staining.

Intradermal treatment with bleomycin

Bleomycin (Nippon Kayaku, Tokyo, Japan) was dissolved in PBS at a concentration of 1mg/ml and was sterilized by filtration. Bleomycin (300μg) or PBS was injected intradermally into the shaved backs of 6 wk-old BALB/c mice 6 times per week for a month, as described previously (26–29). Injections were performed using a 27-gauge needle. The back skin was removed on the day after the final injection. Then, the skin samples were fixed in 10% formalin solution, and embedded in paraffin. Sections were stained with H&E. The dermal thickness was evaluated by measuring the distance between the epidermal-dermal junction and the dermal-fat junction in H&E sections under 100-fold magnification by 2 investigators (H.K. and W.N.) in a blinded manner.

Hydroxyproline assay

To estimate collagen production indirectly, the level of hydroxyproline in the skin tissue was determined by the QuickZyme Hydroxyproline Assay (QuickZyme Biosciences, the Netherlands) according to the manufacturer's instructions (30). Briefly, the skin tissue was acid hydrolyzed by 6M HCl. The hydroxyproline content was then assessed by spectrophotometry at 570nm.

Collagen assay

The amount of collagen in the skin paraffin sections was quantified using Semi-Quantitative Collagen Assay Kit (Chondrex, Redmond, WA). After being dewaxed in xylene and rehydrated in graded alcohols, sections (20 μm in thickness) were immersed in staining solution at room temperature for 30 min. The staining solution was removed, and bleaching solution was added to measure the absorbance at 540 nm and 605 nm in ND-1000 spectrophotometer (NanoDrop technologies, Wilmington, DE). The collagen concentration was calculated based on the following formula: Collagen (μg / section) = $(OD_{540} - (OD_{605} \times 0.291)) / 37.8 \times 1000$ (31).

Statistical analysis

The data presented as bar graphs are the means ± SE of at least three independent experiments. The statistical analysis was carried out with Mann-Whitney *U* test for the comparison of the medians, and Fisher's exact probability test for the analysis of the frequencies. The *p* values <0.05 were considered to be significant.

Results

EBI3 downregulated the collagen expression in normal fibroblasts

As an initial experiment, we examined the effects of the IL-12 family cytokines (Fig. 1A) on the collagen expression in normal fibroblasts by immunoblotting. The protein synthesis of type I collagen was increased slightly by IL-12, whereas it was decreased by IL-23 and IL-35 (Fig. 1B). IL-27 did not alter the collagen expression. Furthermore, we also determined whether each subunit of the IL-12 family affects the collagen levels. Type I collagen expression was not affected by p19, p28 p35, and p40 (Fig. 1C). On the other hand, we found that collagen protein was decreased only by EBI3 (Fig. 1D), which occurred in a dose-dependent manner in the presence or absence of coincubation with TGF-β1. These effects of EBI3 on type I collagen expression and levels of C-terminal propeptides of type I collagen (PIPC) were statistically significant (Fig. 1E).

EBI3 downregulated the stability of collagen mRNA

Accordingly, we focused on the effects of EBI3 on the ECM expression. We performed a PCR array of 84 ECM-related genes

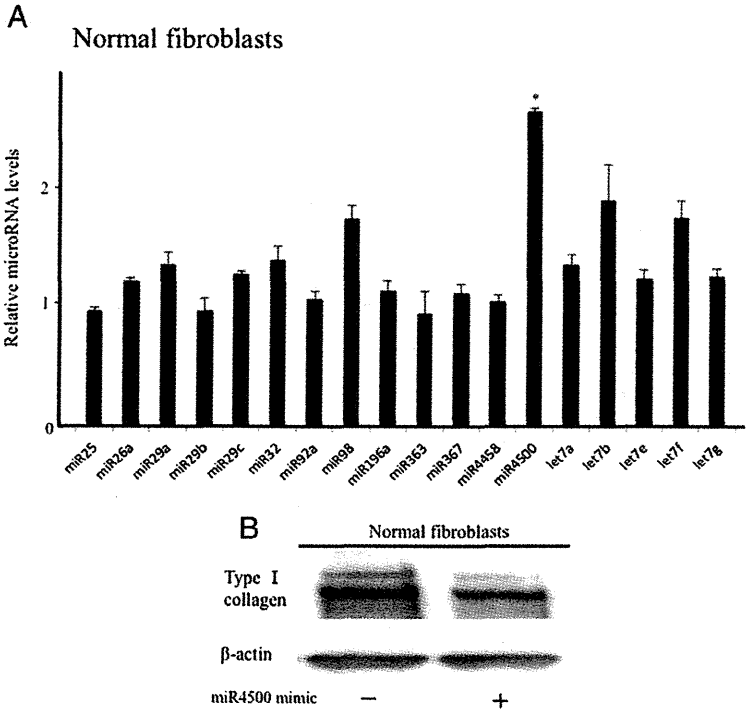

FIGURE 3. The effects of miR-4500 on the collagen expression in normal fibroblasts. (**A**) Normal fibroblasts ($n = 5$) were serum-starved for 24 h and were treated with EBI3 (100 ng/ml) for 12 h. The total miRNA was extracted, and the relative levels of type I collagen-related miRNAs were determined by real-time PCR (normalized to U6). The bar graph represents the fold-stimulation of miRNA expression in EBI3-stimulated cells relative to that in control cells (1.0). $*p < 0.05$. (**B**) Normal fibroblasts at a density of 1×10^5 cells/well in 24-well culture plates were transfected with control miRNA mimic or miR-4500 mimic for 48 h. Cell lysates were then subjected to immunoblotting. A representative result of three independent experiments is shown.

using RNA obtained from dermal fibroblasts stimulated with or without EBI3 for 12 h. When a 2-fold difference determined by the ΔΔCt method was considered meaningful, 18 of the 84 genes were upregulated and 22 genes were downregulated in EBI3-treated fibroblasts in comparison with untreated cells (complete dataset available at the Gene Expression Omnibus microarray data repository, http://www.ncbi.nlm.nih.gov/geo/, accession number GSE68649). Among them, for example, TIMP1 expression was upregulated by EBI3 in the array, however, the increase became insignificant in the real-time PCR results with more samples (n = 3; Fig. 2A). The list of genes up- or downregulated in the EBI3-treated cells both by the PCR array and by real-time PCR for validation are shown in Supplemental Table I; genes that could not be confirmed by real-time PCR were excluded from the list. In the array, the expression of human α2(I) and α1(III) collagen gene was decreased by EBI3 (0.38- and 0.08-fold, respectively). Consistently, quantitative real-time PCR using specific primers for α2(I) and α1(III) collagen as well as α1(I) collagen showed that the mRNA expression of these collagens was significantly reduced by EBI3 in the presence or absence of coincubation with TGF-β1 (Fig. 2B).

To determine whether the downregulation of type I collagen by EBI3 takes place at the transcriptional level or translational level, the stability of type I collagen mRNA and protein was examined.

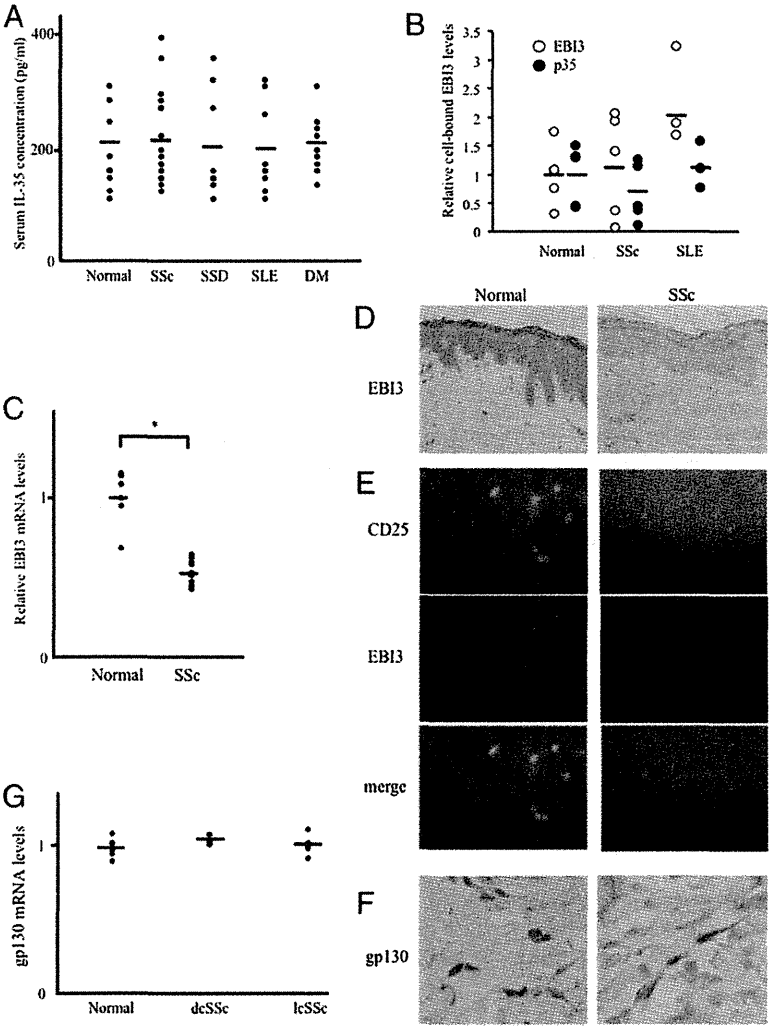

FIGURE 4. The in vivo expression of IL-35 and EBI3. (**A**) The serum IL-35 levels in patients with rheumatic diseases. Serum samples were obtained from patients with SSc (n = 33), scleroderma spectrum disorder (SSD, n = 9), systemic lupus erythematosus (SLE, n = 10) or dermatomyositis (DM, n = 12), and from normal subjects (n = 15). The IL-35 concentrations were determined by ELISA kit. The bars show the mean of each group. (**B**) Cell-bound levels of EBI3 or p35 on $CD3^+$ T cells determined by immunofluorescent flow cytometry in patients with rheumatic diseases. PBMC samples were obtained from patients with SSc (n = 5), systemic lupus erythematosus (SLE, n = 3) and from normal subjects (n = 5). The relative mean fluorescent intensity of EBI3 (white circles) and p35 (black circles) are shown on the ordinate. The bars show the means. The mean values in the samples from normal subjects were set at 1. (**C**) Total RNA was extracted from skin tissue samples derived from 12 patients with SSc and 6 normal subjects. The quantitative real-time PCR was performed to determine the mRNA expression of EBI3. The mean value in samples from normal subjects was set at 1. *$p < 0.05$. (**D**) Paraffin sections were subjected to an immunohistochemical analysis of EBI3 expression. Normal human skin (*left panel*) and SSc-involved skin (*right panel*), original magnification ×200. Representative results of 5 normal and 5 SSc skin samples are shown. (**E**) Sections of normal skin (*left*) or SSc–involved skin (*right*) were costained immunofluorescently with Abs against CD25 (green) and EBI3 (red). Representative results of 5 normal and 5 SSc skin samples are shown. (**F**) Paraffin sections were subjected to an immunohistochemical analysis for gp130 expression. Normal human skin (*left panel*) and SSc-involved skin (*right panel*), original magnification ×400. Representative results of 5 normal and SSc skin samples are shown. (**G**) Total RNA was extracted from skin tissues derived from 12 SSc patients and 6 normal subjects. The quantitative real-time PCR was performed to determine the mRNA expression of gp130. The mean value in samples from normal subjects was set at 1.

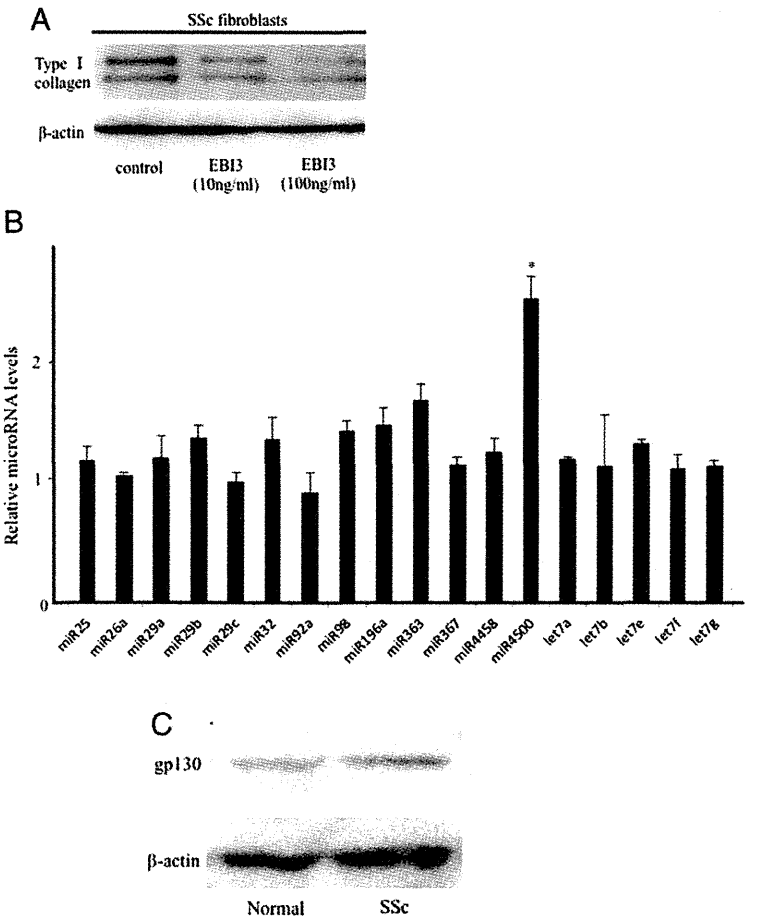

FIGURE 5. The effects of EBI3 on the type I collagen expression in SSc fibroblasts. (**A**) SSc fibroblasts were treated with EBI3 (100 ng/ml) for 24 h. Immunoblotting was performed using Abs against type I collagen and β-actin. A representative result of 3 independent experiments is shown. (**B**) SSc fibroblasts were treated with EBI3 (100 ng/ml) for 12 h. Real-time PCR of type I collagen-related miRNAs was performed as described in Fig. 3A ($n = 3$). (**C**) SSc fibroblasts, at a density of 1×10^5 cells/well in 24-well culture plates, were transfected with control miRNA mimic or miR-4500 mimic for 48 h. Cell lysates were then subjected to immunoblotting. A representative result of three independent experiments is shown.

Because the steady-state level of mRNA is controlled by the level of gene transcription and/or the stability of the mRNA, de novo mRNA synthesis was blocked by actinomycin D, a RNA synthesis inhibitor, in normal fibroblasts in the presence or absence of EBI3 to specifically assess the mRNA stability. As shown in Fig. 2C, the decreased ratio of α2(I) collagen mRNA in the presence of EBI3 was significantly higher than that in the absence of EBI3. On the other hand, when de novo protein synthesis was blocked with cycloheximide, EBI3 stimulation had little effect on the protein half-lives of type I collagen (Fig. 2D). Taken together, these results suggest that the downregulation of type I collagen by EBI3 may be due to the decreased stability of collagen mRNA. Consistent with these results, the promoter activities of serial 5′-deletions of α2(I) collagen promoter construct linked to a CAT reporter gene were not significantly altered by EBI3 (Fig. 2E).

We expected that miRNAs would be involved in the decreased collagen mRNA stability by EBI3 treatment. Among the 18 miRNAs that are thought to target α1(I) and/or α2(I) chains of type I collagen based on TargetScan version 6.2 (http://www.targetscan.org), we found that only the expression of miR-4500 was significantly increased by EBI3 (Fig. 3A). The expression of both α1(I) and α2(I) collagen protein was suppressed by transient transfection with miR-4500 mimic (Fig. 3B). Taken together, these results suggested that EBI3 decreased the type I collagen mRNA expression by inducing miR-4500.

Expression of IL-35 and EBI3 in the sera and involved skin of SSc patients

Next, we measured the serum levels of IL-35 in patients with various rheumatic diseases by ELISA. As shown in Fig. 4A, the mean serum IL-35 levels in patients with SSc, SSD, SLE and DM were not significantly different compared with those in normal subjects. Supplemental Table II shows the association of the serum IL-35 levels with the clinical and laboratory features in SSc patients. Patients with decreased IL-35 levels (below the average of normal subjects) had a significantly higher prevalence of telangiectasia than those with normal levels (35.3% versus 6.3%, $p < 0.05$). A flow cytometric analysis also showed that the levels of p35 bound on CD3+ T cells did not differ among normal subjects, SSc patients and SLE patients (Fig. 4B). The levels of EBI3 bound on T cells were slightly increased in SLE patients, but not statistically significant. Accordingly, the levels of circulating and cell-bound IL-35 were comparable in normal subjects and SSc patients.

In contrast, EBI3 mRNA expression in the involved skin of SSc in vivo determined by real-time PCR was significantly lower than that in normal skin (Fig. 4C). A major source of IL-35 is thought to be regulatory T cells (Treg), and there are several reports indicating that Treg is decreased in SSc skin (32, 33). Consistently, immunohistochemical staining using paraffin-embedded skin sections showed that the expression of EBI3 protein was detected in the keratinocytes of the epidermis and infiltrated cells of the dermis in normal skin, but was hardly detected in the skin of SSc patients (Fig. 4D). Furthermore, costaining of EBI3 and CD25 to detect the presence of Tregs and to identify the cellular source of EBI3 indicated fewer Treg (green) and EBI3-positive cells (red) in SSc dermis, and the colocalization of these proteins (Fig. 4E). Thus, EBI3 may be expressed in keratinocytes and Tregs of SSc-involved skin and may be constitutively decreased. Furthermore, immunostaining revealed that gp130 protein was expressed to

a similar extent in the fibroblast-like spindle-shaped cells of both normal and SSc skin in vivo (Fig. 4F). This result was consistent with similar gp130 mRNA levels between normal and SSc skin by real-time PCR (Fig. 4G). Therefore, dermal fibroblasts may express gp130, and its level was not different between normal and SSc fibroblasts.

EBI3 downregulated the collagen expression in SSc fibroblasts

Not only in normal fibroblasts (Figs. 1–3), but also in cultured SSc dermal fibroblasts, EBI3 downregulated the collagen (Fig. 5A) and upregulated the miR-4500 expression (Fig. 5B). Consistent with the in vivo results (Fig. 4), there were no differences in the gp130 expression between normal and SSc fibroblasts in vitro (Fig. 5C). Taken together, these findings indicate that EBI3 may have an inhibitory effect on the type I collagen expression, and the decreased EBI3 levels in SSc skin (but not SSc sera) contribute to the increased collagen accumulation and tissue fibrosis.

Effects of EBI3 on the skin fibrosis induced by bleomycin in mice

The skin fibrosis induced by bleomycin injection in mice has been used as a murine model of SSc. The skin of control mice expressed EBI3, while the EBI3 expression was decreased in mice with bleomycin-induced skin fibrosis (Fig. 6A), as seen in SSc skin (Fig. 4C, 4D). Accordingly, we tried to determine whether EBI3 supplementation could improve the skin fibrosis in this mouse model of SSc. Bleomycin (300 μg) or PBS (as a control) was locally injected in the backs of BALB/c mice 6 times per week for one month, and at the same time, PBS or EBI3 (3.5μg) was also injected once per week (4 times per month) (Fig. 6B). In the absence of bleomycin injections, EBI3 slightly reduced the dermal thickness (Fig. 6C). Bleomycin treatment without EBI3 induced dermal fibrosis, with more thickened collagen bundles. However, EBI3 decreased the bleomycin-induced dermal thickening. We found the improvement of dermal thickening by EBI3 treatment was statistically significant (Fig. 6D). In addition, increased expression of α1(I) and α2(I) collagen as well as an increased amount of hydroxyproline and collagen in the skin tissue section by bleomycin was also significantly decreased by EBI3 (Fig. 6E). Taken together, these findings indicate that EBI3 supplementation could attenuate the skin fibrosis induced by bleomycin through downregulating collagen.

Discussion

In this study, we examined the involvement of the IL-12 family cytokines in the expression of the ECM. Among the various molecules examined, IL-35 decreased the collagen expression. IL-35 is a novel IL-12 family cytokine produced by Treg, but not by resting or activated effector T cells. IL-35 is thought to mediate the immune suppressive function of Tregs by maintaining self-tolerance and preventing autoimmunity: for example, the depletion of either IL-35 subunit (p35 or EBI3) in Tregs reduced their ability to suppress the inflammation in inflammatory bowel disease model mice (34).

Among the various subunits of the IL-12 family, of note, EBI3 affected the collagen expression in a dose-dependent manner in vitro. In general, a subunit itself has no biological activity.

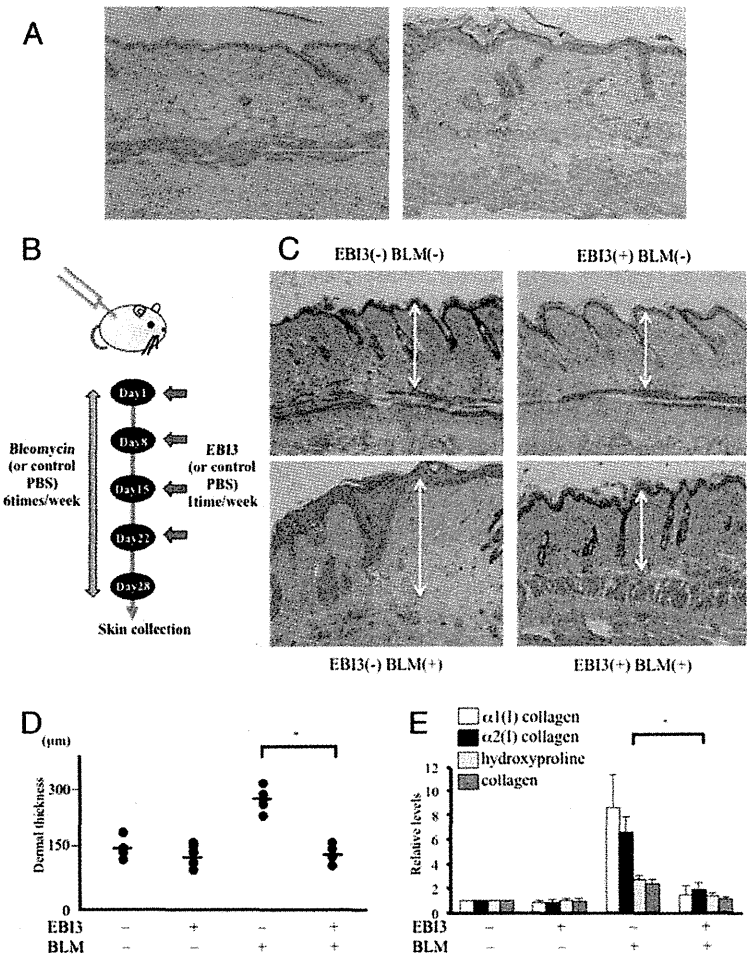

FIGURE 6. Effects of EBI3 on bleomycin (BLM)-induced skin fibrosis in vivo. (**A**) Paraffin sections of mouse skin were subjected to an immunohistochemical analysis for EBI3. (*Left panel*) A PBS-treated wild-type mouse, (*right panel*) bleomycin-treated mouse, original magnification ×200. A representative result of 5 samples is shown. (**B**) The protocol for (**C**)–(**E**) is shown. Bleomycin (300 μg) or a control (PBS) was locally injected into the back skin of the BALB/c mice 6 times per week for a month. At the same time, the control (PBS) or EBI3 (3.5 μg) was also injected into the back skin once per week (total of 4 times a month). The back skin was obtained one day after the final bleomycin injection. (C) H&E staining of PBS- or bleomycin-treated mouse skin injected with the control (PBS) (*left*) or EBI3 (*right*). Scale bar, 0.1 mm. A representative result of 5 samples is shown. (D) The dermal thickness was measured in the PBS- and bleomycin-treated mouse skin injected with control PBS or EBI3. The data are shown on the ordinate (n = 5). The bars show the means. *$p < 0.05$. (E) The mRNA levels of α(I) collagen (white bars) and α2(I) collagen (black bars) in the PBS- and bleomycin-treated mouse skin injected with control PBS or EBI3 were determined by real-time PCR (n = 5). The amount of hydroxyproline (light gray bars) and collagen content (dark gray bars) in the skin sections were quantified using assay kits. The mean values of untreated skin were set at 1. *$p < 0.05$.

Although IL-12 and IL-23 increased and decreased the collagen expression, respectively, their subunits did not have any effect on the collagen expression. These other subunits may therefore exert effects only when they form heterodimers. The reason why EBI3 itself can affect ECM expression is currently unknown, however, EBI3 may form a complex with endogenous p35 or other proteins after its addition to the cell culture medium. Further studies are needed to clarify this point.

IL-35 expression has been thought to be specific to Tregs, because EBI3 is a downstream target of Foxp3 (35). However, according to recent reports, EBI3 is also expressed in other cell types, including intestinal epithelium and aortic smooth muscle cells (36, 37). Our results suggested that epidermal keratinocytes as well as Treg express EBI3, and this expression was decreased in the SSc skin. IL-35 was also reported to induce the proliferation of Treg populations, but suppress Th17 cell development (38). We have previously reported an increase of IL-17 expression in SSc patients (39). The decrease of EBI3 may also contribute to the induction of IL-17.

We demonstrated that the supplementation of EBI3 inhibited bleomycin-induced skin fibrosis in a mouse model, which indicates the therapeutic potential of EBI3 for the fibrotic condition of SSc. To date, corticosteroids, cyclophosphamide and methotrexate are considered to be the first-choice drugs against the severe skin fibrosis of SSc (40, 41). However, these conventional treatments usually have limited effects. Furthermore, these treatments are often accompanied with various significant adverse effects (42). Treatment with the EBI3 subunit may lead to fewer adverse effects than treatment with the IL-35 heterodimer, because EBI3 treatment may have more specific effect on fibrosis. Furthermore, because the EBI3 level was decreased in the SSc epidermis, the local supplementation of EBI3 using an ointment or microinjection into the epidermis may be sufficient, and would further reduce the possibility of side effects. One potential limitation associated with this study is that our results indicated that EBI3 can prevent bleomycin-induced fibrosis, but we did not show the effect of EBI3 on postfibrotic skin by bleomycin, which is the more realistic clinical scenario. Furthermore, Yamamoto et al. reported that C3H/HeJ mice are more sensitive to bleomycin than BALB/c mice (26–28). We used BALB/c mice because this mouse strain was available in our laboratory and because effects of cytokines have been tested in bleomycin-treated BALB/c mice in several papers (43–45), however, the effect of EBI3 and bleomycin should also be examined in other mice strains. Future studies should focus on clarifying these points, which may lead to a better understanding of this disease and new therapeutic strategies.

Disclosures

The authors have no financial conflicts of interest.

References

1. Uitto, J., and D. Kouba. 2000. Cytokine modulation of extracellular matrix gene expression: relevance to fibrotic skin diseases. *J. Dermatol. Sci.* 24(Suppl. 1): S60–S69.
2. Trojanowska, M., E. C. LeRoy, B. Eckes, and T. Krieg. 1998. Pathogenesis of fibrosis: type I collagen and the skin. *J. Mol. Med.* 76: 266–274.
3. Varga, J., and D. Abraham. 2007. Systemic sclerosis: a prototypic multisystem fibrotic disorder. *J. Clin. Invest.* 117: 557–567.
4. Gabrielli, A., E. V. Avvedimento, and T. Krieg. 2009. Scleroderma. *N. Engl. J. Med.* 360: 1989–2003.
5. Ihn, H., K. Yamane, M. Kubo, and K. Tamaki. 2001. Blockade of endogenous transforming growth factor β signaling prevents up-regulated collagen synthesis in scleroderma fibroblasts: association with increased expression of transforming growth factor β receptors. *Arthritis Rheum.* 44: 474–480.
6. Asano, Y., H. Ihn, K. Yamane, M. Kubo, and K. Tamaki. 2004. Impaired Smad7-Smurf-mediated negative regulation of TGF-β signaling in scleroderma fibroblasts. *J. Clin. Invest.* 113: 253–264.
7. Takehara, K. 2003. Hypothesis: pathogenesis of systemic sclerosis. *J. Rheumatol.* 30: 755–759.
8. Overbeck, M. J., A. Boonstra, A. E. Voskuyl, M. C. Vonk, A. Vonk-Noordegraaf, M. P. van Berkel, W. J. Mooi, B. A. Dijkmans, L. S. Hondema, E. F. Smit, and K. Grünberg. 2011. Platelet-derived growth factor receptor-β and epidermal growth factor receptor in pulmonary vasculature of systemic sclerosis-associated pulmonary arterial hypertension versus idiopathic pulmonary arterial hypertension and pulmonary veno-occlusive disease: a case-control study. *Arthritis Res. Ther.* 13: R61.
9. Brissett, M., K. L. Veraldi, J. M. Pilewski, T. A. Medsger, Jr., and C. A. Feghali-Bostwick. 2012. Localized expression of tenascin in systemic sclerosis-associated pulmonary fibrosis and its regulation by insulin-like growth factor binding protein 3. *Arthritis Rheum.* 64: 272–280.
10. Kawaguchi, Y. 1994. IL-1 α gene expression and protein production by fibroblasts from patients with systemic sclerosis. *Clin. Exp. Immunol.* 97: 445–450.
11. Feghali, C. A., K. L. Bost, D. W. Boulware, and L. S. Levy. 1992. Mechanisms of pathogenesis in scleroderma. I. Overproduction of interleukin 6 by fibroblasts cultured from affected skin sites of patients with scleroderma. *J. Rheumatol.* 19: 1207–1211.
12. Makino, T., S. Fukushima, S. Wakasugi, and H. Ihn. 2009. Decreased serum IL-7 levels in patients with systemic sclerosis. *Clin. Exp. Rheumatol.* 27(3Suppl. 54): 68–69.
13. Subcommittee for scleroderma criteria of the American Rheumatism Association Diagnostic and Therapeutic Criteria Committee. 1980. Preliminary criteria for the classification of systemic sclerosis (scleroderma). *Arthritis Rheum.* 23: 581–590.
14. Maricq, H. R., M. C. Weinrich, J. E. Keil, E. A. Smith, F. E. Harper, A. I. Nussbaum, E. C. LeRoy, A. R. McGregor, F. Diat, and E. J. Rosal. 1989. Prevalence of scleroderma spectrum disorders in the general population of South Carolina. *Arthritis Rheum.* 32: 998–1006.
15. Maricq, H. R., A. R. McGregor, F. Diat, E. A. Smith, D. B. Maxwell, E. C. LeRoy, and M. C. Weinrich. 1990. Major clinical diagnoses found among patients with Raynaud phenomenon from the general population. *J. Rheumatol.* 17: 1171–1176.
16. Ihn, H., S. Sato, T. Tamaki, Y. Soma, T. Tsuchida, Y. Ishibashi, and K. Takehara. 1992. Clinical evaluation of scleroderma spectrum disorders using a points system. *Arch. Dermatol. Res.* 284: 391–395.
17. Higashi-Kuwata, N., M. Jinnin, T. Makino, S. Fukushima, Y. Inoue, F. C. Muchemwa, Y. Yonemura, Y. Komohara, M. Takeya, H. Mitsuya, and H. Ihn. 2010. Characterization of monocyte/macrophage subsets in the skin and peripheral blood derived from patients with systemic sclerosis. *Arthritis Res. Ther.* 12: R128.
18. Wang, R. X., C. R. Yu, I. M. Dambuza, R. M. Mahdi, M. B. Dolinska, Y. V. Sergeev, P. T. Wingfield, S. H. Kim, and C. E. Egwuagu. 2014. Interleukin-35 induces regulatory B cells that suppress autoimmune disease. *Nat. Med.* 20: 633–641.
19. Honda, N., M. Jinnin, T. Kira-Etoh, K. Makino, I. Kajihara, T. Makino, S. Fukushima, Y. Inoue, Y. Okamoto, M. Hasegawa, et al. 2013. miR-150 down-regulation contributes to the constitutive type I collagen overexpression in scleroderma dermal fibroblasts via the induction of integrin β3. *Am. J. Pathol.* 182: 206–216.
20. Trappoliere, M., A. Caligiuri, M. Schmid, C. Bertolani, P. Failli, F. Vizzutti, E. Novo, C. di Manzano, F. Marra, C. Loguercio, and M. Pinzani. 2009. Silybin, a component of sylimarin, exerts anti-inflammatory and anti-fibrogenic effects on human hepatic stellate cells. *J. Hepatol.* 50: 1102–1111.
21. Jinnin, M., T. Makino, I. Kajihara, N. Honda, K. Makino, A. Ogata, and H. Ihn. 2010. Serum levels of soluble vascular endothelial growth factor receptor-2 in patients with systemic sclerosis. *Br. J. Dermatol.* 162: 751–758.
22. Ihn, H., K. Ohnishi, T. Tamaki, E. C. LeRoy, and M. Trojanowska. 1996. Transcriptional regulation of the human α2(I) collagen gene. Combined action of upstream stimulatory and inhibitory cis-acting elements. *J. Biol. Chem.* 271: 26717–26723.
23. Filippova, M., H. Song, J. L. Connolly, T. S. Dermody, and P. J. Duerksen-Hughes. 2002. The human papillomavirus 16 E6 protein binds to tumor necrosis factor (TNF) R1 and protects cells from TNF-induced apoptosis. *J. Biol. Chem.* 277: 21730–21739.
24. Ma, J., and L. Z. Xie. 2013. [Eukaryotic expression and biological activity of human interleukin-35]. *Zhongguo Yi Xue Ke Xue Yuan Xue Bao* 35: 618–622.
25. Jinnin, M., D. Medici, L. Park, N. Limaye, Y. Liu, E. Boscolo, J. Bischoff, M. Vikkula, E. Boye, and B. R. Olsen. 2008. Suppressed NFAT-dependent VEGFR1 expression and constitutive VEGFR2 signaling in infantile hemangioma. *Nat. Med.* 14: 1236–1246.
26. Yamamoto, T., S. Takagawa, I. Katayama, K. Yamazaki, Y. Hamazaki, H. Shinkai, and K. Nishioka. 1999. Animal model of sclerotic skin. I: Local injections of bleomycin induce sclerotic skin mimicking scleroderma. *J. Invest. Dermatol.* 112: 456–462.
27. Yamamoto, T., M. Kuroda, and K. Nishioka. 2000. Animal model of sclerotic skin. III: Histopathological comparison of bleomycin-induced scleroderma in various mice strains. *Arch. Dermatol. Res.* 292: 535–541.
28. Oi, M., T. Yamamoto, and K. Nishioka. 2004. Increased expression of TGF-beta1 in the sclerotic skin in bleomycin-'susceptible' mouse strains. *J. Med. Dent. Sci.* 51: 7–17.
29. Tanaka, C., M. Fujimoto, Y. Hamaguchi, S. Sato, K. Takehara, and M. Hasegawa. 2010. Inducible costimulator ligand regulates bleomycin-induced lung and skin fibrosis in a mouse model independently of the inducible costimulator/inducible costimulator ligand pathway. *Arthritis Rheum.* 62: 1723–1732.
30. Probert, P. M. E., M. R. Ebrahimkhani, F. Oakley, M. Mann, A. D. Burt, and D. A. Mann, and M. C. Wright. 2014. A reversible model for periportal fibrosis and a refined alternative to bile duct ligation. *Toxicol. Res.* 3: 98–109.

31. Marotta, M., and G. Martino. 1985. Sensitive spectrophotometric method for the quantitative estimation of collagen. *Anal. Biochem.* 150: 86–90.
32. Antiga, E., P. Quaglino, S. Bellandi, W. Volpi, E. Del Bianco, A. Comessatti, S. Osella-Abate, C. De Simone, A. Marzano, M. G. Bernengo, et al. 2010. Regulatory T cells in the skin lesions and blood of patients with systemic sclerosis and morphoea. *Br. J. Dermatol.* 162: 1056–1063.
33. Klein, S., C. C. Kretz, V. Ruland, C. Stumpf, M. Haust, W. Hartschuh, M. Hartmann, A. Enk, E. Suri-Payer, N. Oberle, et al. 2011. Reduction of regulatory T cells in skin lesions but not in peripheral blood of patients with systemic scleroderma. *Ann. Rheum. Dis.* 70: 1475–1481.
34. Neurath, M. F. 2008. IL-12 family members in experimental colitis. *Mucosal Immunol.* 1(Suppl. 1): S28–S30.
35. Seyerl, M., S. Kirchberger, O. Majdic, J. Seipelt, C. Jindra, C. Schrauf, and J. Stöckl. 2010. Human rhinoviruses induce IL-35-producing Treg via induction of B7-H1 (CD274) and sialoadhesin (CD169) on DC. *Eur. J. Immunol.* 40: 321–329.
36. Maaser, C., L. J. Egan, M. P. Birkenbach, L. Eckmann, and M. F. Kagnoff. 2004. Expression of Epstein-Barr virus-induced gene 3 and other interleukin-12-related molecules by human intestinal epithelium. *Immunology* 112: 437–445.
37. Kempe, S., P. Heinz, E. Kokai, O. Devergne, N. Marx, and T. Wirth. 2009. Epstein-barr virus-induced gene-3 is expressed in human atheroma plaques. *Am. J. Pathol.* 175: 440–447.
38. Niedbala, W., X. Q. Wei, B. Cai, A. J. Hueber, B. P. Leung, I. B. McInnes, and F. Y. Liew. 2007. IL-35 is a novel cytokine with therapeutic effects against collagen-induced arthritis through the expansion of regulatory T cells and suppression of Th17 cells. *Eur. J. Immunol.* 37: 3021–3029.
39. Nakashima, T., M. Jinnin, K. Yamane, N. Honda, I. Kajihara, T. Makino, S. Masuguchi, S. Fukushima, Y. Okamoto, M. Hasegawa, et al. 2012. Impaired IL-17 signaling pathway contributes to the increased collagen expression in scleroderma fibroblasts. *J. Immunol.* 188: 3573–3583.
40. Apras, S., I. Ertenli, Z. Ozbalkan, S. Kiraz, M. A. Ozturk, I. C. Haznedaroglu, V. Cobankara, S. Pay, and M. Calguneri. 2003. Effects of oral cyclophosphamide and prednisolone therapy on the endothelial functions and clinical findings in patients with early diffuse systemic sclerosis. *Arthritis Rheum.* 48: 2256–2261.
41. Pope, J. E., N. Bellamy, J. R. Seibold, M. Baron, M. Ellman, S. Carette, C. D. Smith, I. M. Chalmers, P. Hong, D. O'Hanlon, et al. 2001. A randomized, controlled trial of methotrexate versus placebo in early diffuse scleroderma. *Arthritis Rheum.* 44: 1351–1358.
42. Haustein, U. F. 2002. Systemic sclerosis-scleroderma. *Dermatol. Online J.* 8: 3.
43. Yamamoto, T., S. Takagawa, M. Kuroda, and K. Nishioka. 2000. Effect of interferon-gamma on experimental scleroderma induced by bleomycin. *Arch. Dermatol. Res.* 292: 362–365.
44. Koca, S. S., A. Isik, I. H. Ozercan, B. Ustundag, B. Evren, and K. Metin. 2008. Effectiveness of etanercept in bleomycin-induced experimental scleroderma. *Rheumatology (Oxford)* 47: 172–175.
45. Arai, M., Y. Ikawa, S. Chujo, Y. Hamaguchi, W. Ishida, F. Shirasaki, M. Hasegawa, N. Mukaida, M. Fujimoto, and K. Takehara. 2013. Chemokine receptors CCR2 and CX3CR1 regulate skin fibrosis in the mouse model of cytokine-induced systemic sclerosis. *J. Dermatol. Sci.* 69: 250–258.

Journal of Dermatological Science 79 (2015) 268–278

Contents lists available at ScienceDirect

Journal of Dermatological Science

journal homepage: www.jdsjournal.com

Mice overexpressing integrin αv in fibroblasts exhibit dermal thinning of the skin

Zhongzhi Wang[a], Masatoshi Jinnin[a,*], Yuki Kobayashi[a], Hideo Kudo[a], Kuniko Inoue[a], Wakana Nakayama[a], Noritoshi Honda[a], Katsunari Makino[a], Ikko Kajihara[a], Takamitsu Makino[a], Satoshi Fukushima[a], Yutaka Inagaki[b], Hironobu Ihn[a]

[a] Department of Dermatology and Plastic Surgery, Faculty of Life Sciences, Kumamoto University, Honjo 1-1-1, Kumamoto 860-8556, Japan
[b] Center for Matrix Biology and Medicine, Graduate School of Medicine, Tokai University, 143 Shimo-kasuya, Isehara, Kanagawa 259-1193, Japan

ARTICLE INFO

Article history:
Received 27 March 2014
Received in revised form 26 April 2015
Accepted 17 June 2015

Keywords:
Integrin αv
Transgenic mice
MMP-1

ABSTRACT

Background: Integrins, especially αv integrin (ITGAV), are thought to play central roles in tissue fibrosis and the pathogenesis of scleroderma. So far, skin phenotype of tissue-specific transgenic mice of ITGAV have not been investigated.
Objective: To investigate the role of ITGAV in the skin fibrosis, we engineered transgenic mice that overexpress ITGAV in the fibroblasts under the control of the COL1A2 enhancer promoter.
Methods: Protein or RNA expression was evaluated by real-time PCR, immunohistochemistry, immunoblotting and immunoprecipitation.
Results: Dermal thickness and Masson's trichrome staining were decreased in ITGAV transgenic (Tg) mice compared with wild-type (WT) mice. Protein and mRNA levels of COL1A2, COL3A1, CTGF and integrin β3 were down-regulated in the skin of Tg mice. In addition, the cell proliferation of cultured dermal fibroblasts obtained from Tg mice skin was decreased compared to those of WT mice.
FAK phosphorylation was reduced in fibroblasts cultured from Tg mice skin in comparison to WT mice fibroblasts. Integrin β3 siRNA inhibited FAK phosphorylation levels, while FAK inhibitor reduced the expression of collagens and CTGF in mice dermal fibroblasts.
Conclusions: The down-regulation of collagen or CTGF by decreased integrin β3 and FAK phosphorylation may cause the dermal thinning in Tg mice. Lower CTGF may also result in reduced growth of Tg mice fibroblasts. Our hypothesis is that the balance between α and β chain of integrins positively or negatively control collagen expression and dermal thickness. This study gave a new insight in the treatment of tissue fibrosis and scleroderma by balancing integrin expression.

1. Introduction

Integrins are a glycoprotein family of heterodimeric transmembrane receptors that attach cells to extracellular matrix (ECM) or to cell surface ligands. Integrins consists of α and β subunits. To date, 18 α subunits and 8 β subunits are found, which can generate at least 24 different heterodimers.

In mammals, the αv integrin subunit (ITGAV) can form heterodimer with β chains 1,3,5,6, and 8. ITGAV also binds to Arg–Gly–Asp (RGD) motif of fibronectin, vitronectin, osteopontin as well as latency-associated peptide (LAP) of transforming growth factor (TGF)-β1 or -β3. Through such interaction with other molecules, ITGAV have been implicated in various cellular responses to injury, immunity, angiogenesis and tumor progression [1].

Systemic sclerosis (SSc) is an acquired disorder characterized by ECM deposition and tissue fibrosis of skin and internal organs. Although the mechanism of the ECM deposition is still unclear, many of the characteristics of fibroblasts cultured from fibrotic skin of SSc in vitro are similar to those of normal fibroblasts stimulated by TGF-β1. Considering that TGF-β1 is one of the most potent inducers of ECM deposition [2] and that SSc dermal fibroblasts produce excessive amounts of various collagens (especially type I and type III collagens) [3–5], the ECM deposition in SSc may be a result of stimulation by TGF-β1 signaling.

* Corresponding author at: Masatoshi Jinnin (MD, PhD), Department of Dermatology and Plastic Surgery, Faculty of Life Sciences, Kumamoto University, Honjo 1-1-1, Kumamoto 860-8556, Japan. Fax: +81 96 373 5235.
E-mail addresses: mjin@kumamoto-u.ac.jp, jinjin1011@hotmail.com (M. Jinnin).

http://dx.doi.org/10.1016/j.jdermsci.2015.06.008
0923-1811/

Bioactive TGF-β1 usually wrapped by LAP, forming the small latent complex (SLC). LAP prevents bioactive TGF-β1 from binding to its receptors, resulting in the TGF-β1 inactivation. Physical interactions of LAP with integrins lead to the release of bioactive TGF-β1 [6,7]. Previously we showed that active and total (active and latent) TGF-β1 levels in the culture media of SSc fibroblasts are not increased compared to those in normal fibroblasts [8]. Accordingly, the ECM deposition in SSc may be caused by intrinsically activated TGF-β signaling, without increasing the concentration of active TGF-β1. As the mechanisms of activating endogenous latent TGF-β1 in SSc fibroblasts, we have recently reported the overexpression of integrin αvβ5 and αvβ3 in these cells [7,9,10]. These integrins may recruit and activate SLC only in the pericellular region of SSc fibroblasts, which increase the incidence of interaction between active TGF-β1 and its receptors. Therefore, overexpression of integrins, especially ITGAV, is thought to be the most upstream event of TGF-β1 activation and ECM deposition in SSc fibroblasts.

To date, there have been several mice models of skin fibrosis (e.g. bleomycin-injected mice or Fra-2 knockout mice) [11]. However, these mice did not show clinical skin sclerosis but only the histological fibrosis. To develop SSc mice model with apparent skin sclerosis and to investigate the role of ITGAV in the skin fibrosis, we engineered transgenic mice that overexpress ITGAV in the fibroblasts under the control of α2(I) collagen (COL1A2) enhancer promoter (Fig. 1a). However, contrary to our expectation, mice overexpressing ITGAV in fibroblasts exhibit dermal thinning of the skin.

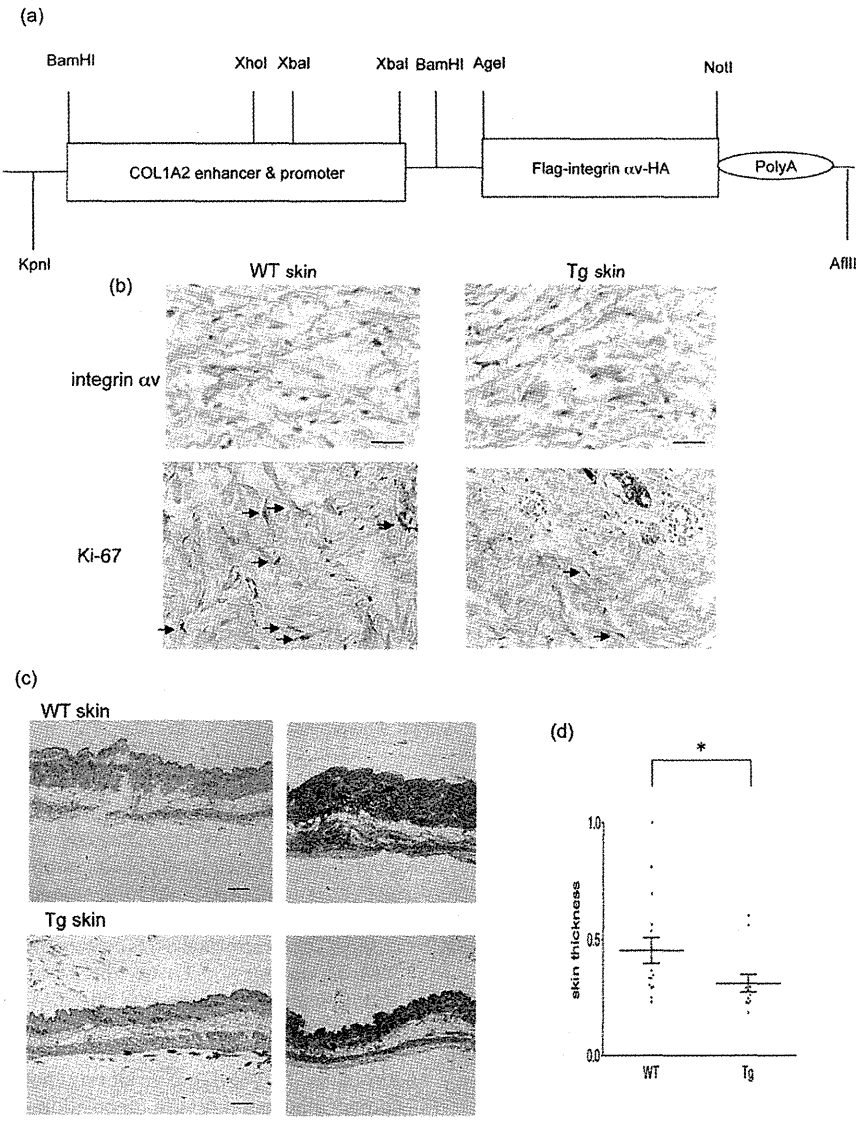

Fig. 1. The expression of integrin αv in the skin of transgenic mice.
(a) Schematic presentation of the transgene construct. The construct consists of a AgeI and NotI fragment containing the entire coding region of integrin αv cDNA with Flag and HA tag under the COL1A2 enhancer promoter followed by a globin poly-A tail.
(b) Paraffin sections of mice skin were subjected to immunohistochemical analysis for HA tag or Ki-67. Representative results of 4 WT mice and 4 Tg mice (male; $n=2$, female; $n=2$) are shown. Scale bar = 20 μm.
(c, d) Hematoxylin and eosin (HE, left panels) and Masson's trichrome staining (right panels). Representative results of WT mice skin (male; $n=6$, female; $n=9$) and Tg mice skin (male; $n=5$, female; $n=7$) are shown. Original magnification × 40. Scale bar = 50 mm (c).
The graph depicts dermal thickness of Tg and WT mice. Bars show means ± SE. $^*p<0.05$ (d).

2. Materials and methods

2.1. Plasmid construction

Full-length mice ITGAV cDNA with a HA or Flag tag at the c-terminus was subcloned into the BamH I and Xha I site of the pEGFP-1-COL1A2 enhancer and promoter vector [12] (Fig. 1a). The construct was sequenced to confirm the orientation.

2.2. Transgenic Mice

pEGFP-1-COL1A2-ITGAV DNA fragment was microinjected into fertilized eggs of C57BL/6 mice to generate transgenic founders. Founders were screened by reverse transcription-PCR (RT-PCR) using primers complementary to ITGAV and Mfe I-coding sequences, as well as Southern blot analysis.

All mice were bred and maintained at the animal facility under specific pathogen-free and temperature-controlled environment with a 12 h light/dark cycle, and were fed a standard diet and water ad libitum. Eight- to 10-week-old mice were used for the experiments. All animal experimental protocols in this study were approved by the Committee on the Animal Research at Kumamoto University. We confirmed that consistent results were obtained in mice derived from at least 3 independent founders in each experiment.

2.3. Histological studies and immunohistochemistry

Tissue samples of mice back skin were fixed in 4% paraformaldehyde for 24 h. The specimens were then embedded in paraffin, sectioned and stained with hematoxylin and eosin (HE) or Masson's trichrome, before being evaluated by light microscopy. Dermal thickness was evaluated by measuring the distance between the epidermal-dermal junction and the dermal-fat junction in HE sections under 100-folds magnification using Digimizer Image Analysis software (MedCalc Software bvba, Ostend, Belgium).

For immunohistochemistry, paraffin-embedded sections were dewaxed in xylene and rehydrated in graded alcohols. The sections were treated with protein K (DakoCytomation, Carpinteria, CA) for 10 min. Immunohistochemistry was performed with HA antibody (Roche, Mannheim, Germany 1:500) or Ki-67 (Abcam, Cambridge, United Kingdom, 1:100).

2.4. Cells

NIH3T3 cell were purchased from ATCC (Manassas, VA). Mouse dermal fibroblasts were cultured from the mice back skin [13]. Primary explant cultures were established in Dulbecco's Modified Eagle Medium (GIBCO, Carlsbad, CA) supplemented with 10% FCS. Fibroblasts between the third and sixth subpassages were used for experiments.

2.5. RNA extraction and real-time PCR analysis

Total RNA was extracted from cultured cells or skin tissues using Isogen (Nippon Gene, Tokyo, Japan). First-strand cDNA was synthesized by PrimeScript RT reagent Kit (Takara, Otsu, Japan). Quantitative real-time PCR used primers and templates mixed with SYBR Premix Ex Taq II Kit (Takara). Primer sets were purchased from Takara. DNA was amplified for 40 cycles of denaturation for 5 s at 95 °C and annealing for 30 s at 60 °C. Transcript level of gene of interest was normalized to that of GAPDH in the same sample.

2.6. Immunoblotting

Cell lysates were obtained from cultured cells and skin tissues using Denaturing Cell Extraction Buffer (Biosource International, Camarillo, CA). Aliquots of the cell lysates (normalized for protein concentrations measured by BCA kit) were separated by electrophoresis on 10% SDS-polyacrylamide gels and transferred onto polyvinylidene difluoride filters. After blocking with 1% milk, the polyvinylidene difluoride filters were then incubated with primary antibodies. The filters were incubated with secondary antibody, and the immunoreactive bands were visualized using Super Signal® West Femto Maximum Sensitivity Substrate (Thermo, Rockford, IL). The density of each band was measured using Quantity One 1D analysis software (version 4.6.6) on ChemiDoc XRS System (Bio-Rad Laboratories, Hercules, CA).

Primary antibodies against integrin β1, β5, paxillin, phospho-paxillin, JNK, and phospho-JNK were purchased from Cell signaling (Beverly, MA). Antibody against MMP-1 or CTGF was from Thermo or Abcam, respectively. Anti-type I or type III collagen antibody was from SouthernBiotech (Birmingham, AL). Anti-ITGAV, integrin β3, β6, β8, smad3, p-smad3, FAK, p-FAK, and β-actin antibodies were from Santa Cruz Biotechnology (Santa Cruz, CA). Precision Plus Protein Standards All Blue (Bio-Rad Laboratories) was used for size marker.

2.7. Biotinylation and immunoprecipitation

After washed with PBS, confluent quiescent cells were incubated with membrane impermeant NHS-LC-Biotin (Pierce, Rockford, IL) dissolved at 0.5 mg/ml in PBS at 4 °C for 30 min. Whole-cell lysates were used for immunoprecipitation as described previously [7]. The immunoprecipitates were subjected to SDS-PAGE, and immunoblotting was performed as described above using antibody against streptavidin coupled to horseradish peroxidase (Santa Cruz Biotechnology).

2.8. Measurement of TGF-β concentrations

Active TGF-β1 levels were measured with specific ELISA kit (Mouse TGFβ1 ELISA Kit, Boster, Fremont, CA). Briefly, antibody for TGF-β1 was precoated onto microtiter wells. Aliquots of sample were treated by activating reagents, and added to each well, followed by biotinylated antibody to TGF-β1. Color was developed with Avidin-Biotin-Peroxidase Complex working solution, and the absorbance at 450 nm was measured. The concentration of TGF-β1 in each sample was determined by interpolation from a standard curve.

2.9. The transient transfection

siRNA against integrin β3 and negative control siRNA were purchased from Santa Cruz Biotechnology. Lipofectamine RNAi-MAX (Invitrogen, Carlsbad, CA) was utilized as a transfection reagent.

siRNAs were mixed with the transfection reagent for reverse transfection, and then added when cells were plated, followed by incubation at 37 °C in 5% CO_2.

2.10. Cell count

Mouse dermal fibroblasts were plated at a density of 10^5 cells/well in 6-well culture plates. After incubation, the cells were detached from the wells by trypsin treatment, and counted using Coulter Counter (Beckman Coulter, Jersey City, NJ).

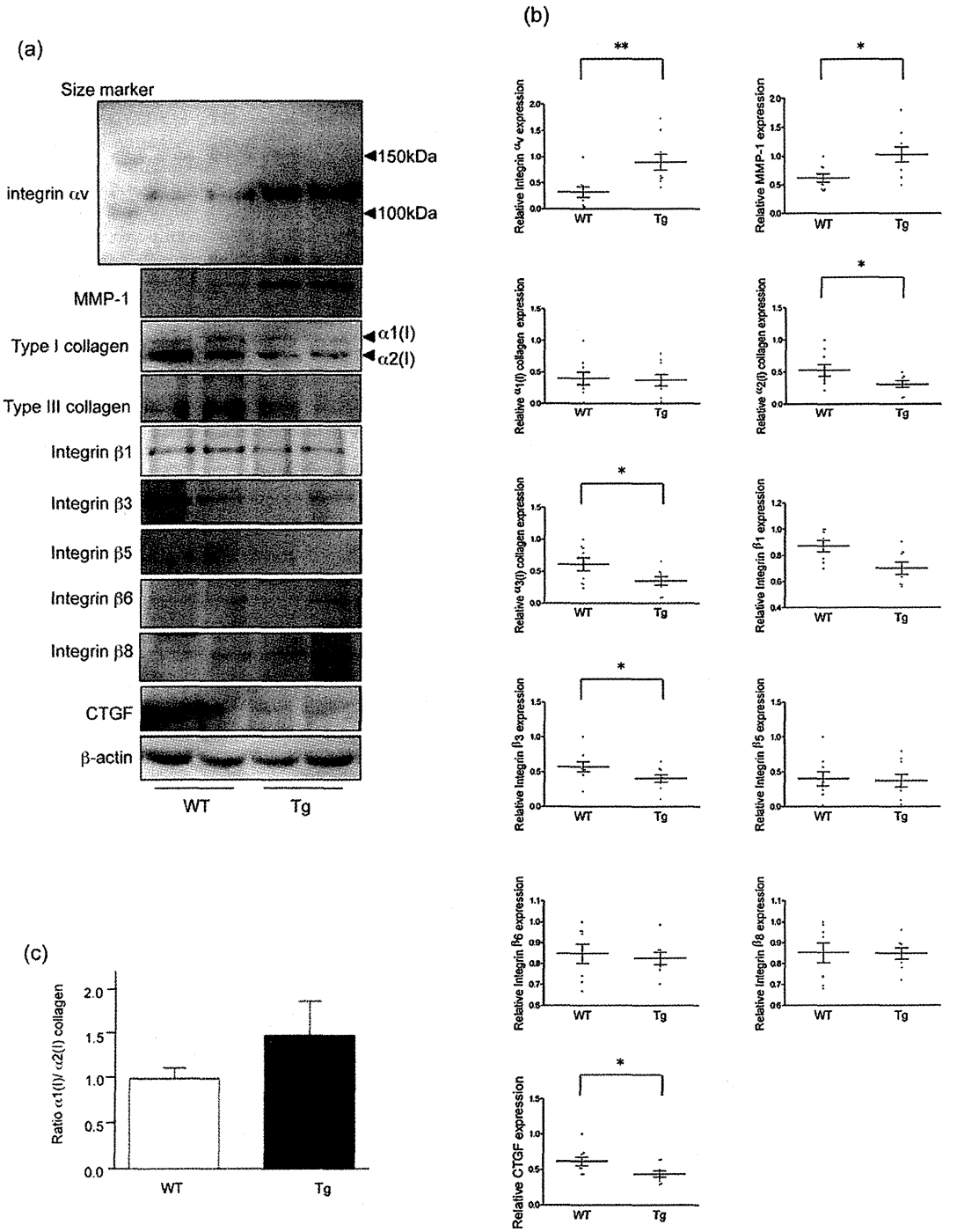

Fig. 2. Protein levels of extracellular matrix-related molecules in the skin of integrin αv transgenic mice in vivo.
Cell lysates obtained from the skin of WT mice and Tg mice were subjected to Immunoblotting. To show the bands for integrin αv protein are the right size (125kDa), size marker was also included in the blot. β-actin levels were shown as controls. Results are representative of 9 WT or Tg mice (male; $n=5$ and female; $n=4$) (a).
The protein levels of each molecule quantitated by scanning densitometry and corrected for the levels of β-actin in the same samples are shown on the ordinate. The maximum level in WT mice was set at 1. Horizontal bars indicate average values. Vertical bars show SE. $^{*}p<0.05$. $^{**}p<0.01$ (b). The ratio of α1(I)/α2(I) collagen was shown in (c). The ratio in WT mice was set at 1.

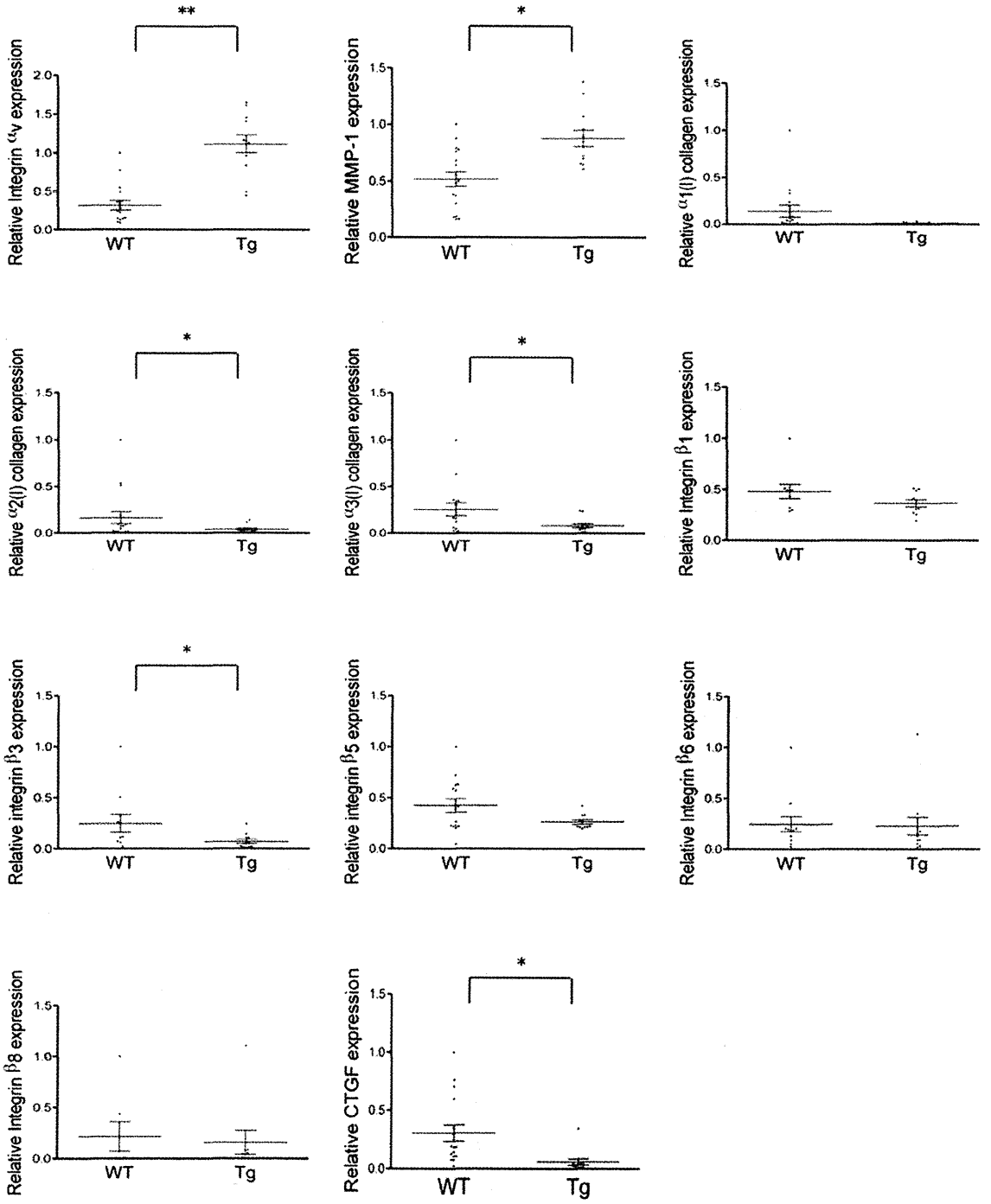

Fig. 3. mRNA levels of extracellular matrix-related molecules in the skin of integrin αv transgenic mice in vivo.
mRNA levels of indicated genes measured by quantitative real-time PCR in the skin of WT mice (male; $n = 6$, female; $n = 9$) and Tg mice (male; $n = 5$, female; $n = 7$) are shown on the ordinate. Bars show means. The maximum values in WT mice were set at 1. $^{*}p < 0.05$, $^{**}p < 0.01$.

2.11. Statistical analysis

All data are expressed as means ± SE. Differences between 2 groups were compared using Mann-Whitney's U test for non-parametric variables by SPSS 17.0 (SPSS Japan Inc., Tokyo, Japan). $p < 0.05$ was considered statistically significant.

3. Results

3.1. Phenotype of transgenic mice overexpressing ITGAV in dermal fibroblasts

As an initial experiment, immunohistochemistry was performed using anti-HA tag antibody to evaluate the expression of

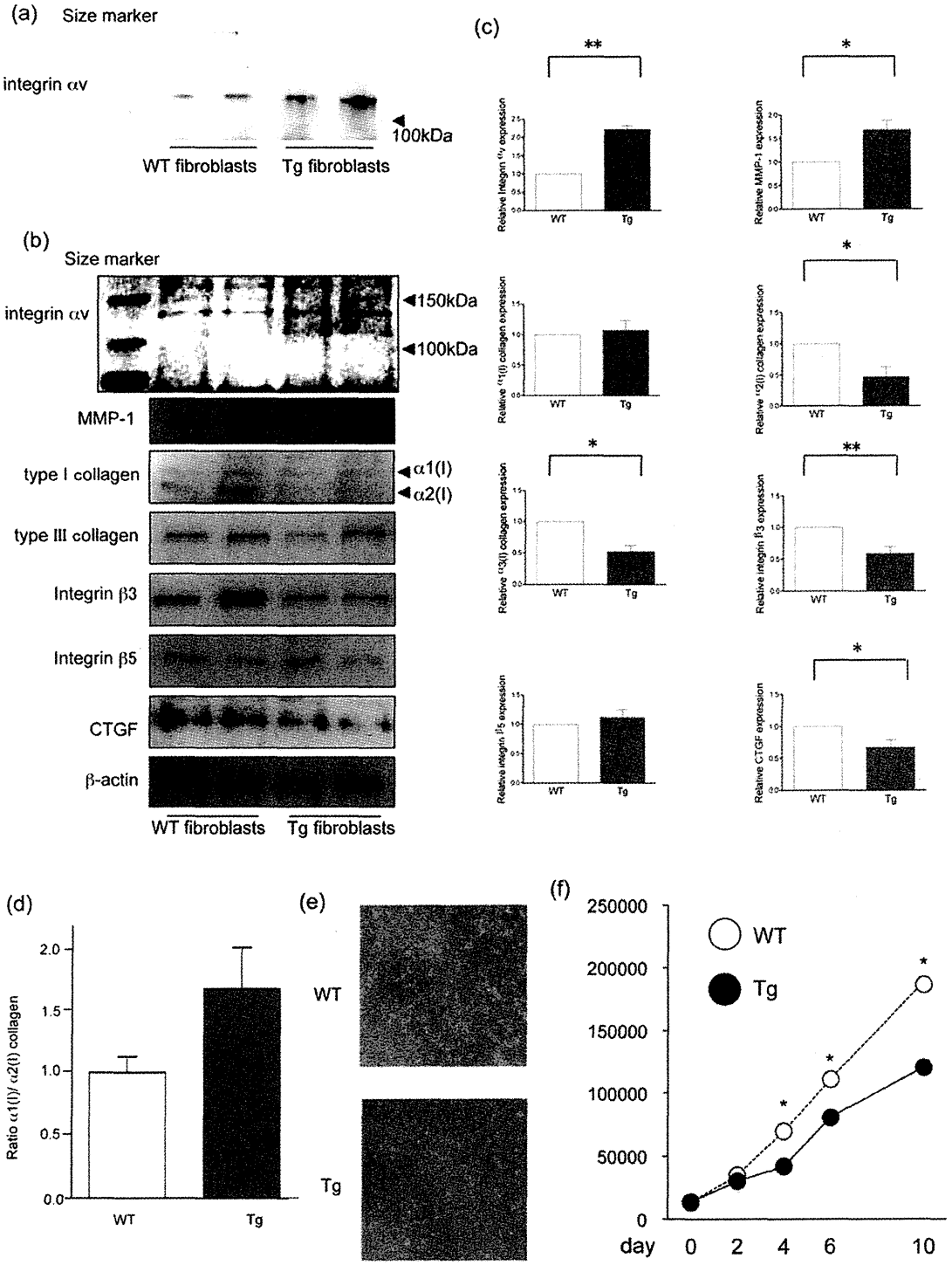

Fig. 4. Protein levels of extracellular matrix-related molecules in cultured mouse dermal fibroblasts.

(a) Cell surface proteins of cultured mouse dermal fibroblasts were labeled with biotin, and cell lysates were immunoprecipitated using anti-integrin αv subunit antibody. One representative of three independent experiments using 2 WT and 2 Tg mice (male; $n=1$, female; $n=1$) is shown. To show the bands for integrin αv protein are the right size (125kDa), size marker was also included in the blot.

(b) Cell lysates of fibroblasts derived from WT mice or Tg mice were subjected to immunoblotting. β-actin levels were shown as controls. Results are representative of 6 WT or Tg mice (male; $n=3$ and female; $n=3$).

(c, d) The mRNA levels of each molecule measured by quantitative real-time PCR using mRNA obtained from dermal fibroblasts of WT mice and Tg mice. Bar graphs depict means + SE of the results in the 6 WT or Tg mice (male; $n=3$ and female; $n=3$). The values of WT mice in each experiment were set at 1, and relative expression levels of indicated genes were presented. $^{*}p<0.05$. $^{**}p<0.01$ (c). The ratio of α1(I)/α2(I) collagen was shown in (d). The ratio in WT mice was set at 1.

(e) Mouse cultured dermal fibroblasts derived from WT mice and Tg mice were incubated for 7 days. Micrographs of cells were shown. Original magnification × 40. One representative of three independent experiments using 2 WT and 2 Tg mice (male; $n=1$, female; $n=1$) is shown.

(f) Cultured dermal fibroblasts derived from WT mice (white circles) and Tg mice (black circles) were incubated for indicated time course. Cell count was performed as described in "Materials and Methods". The y-axis indicates mean cell number. $^{*}p \leq 0.05$ compared with Tg mice fibroblasts.

ITGAV in the skin of ITGAV transgenic (Tg) mice. ITGAV expression was increased in fibroblast-like spindle-shaped cells of Tg mice skin as compared to wild-type (WT) mice skin (Fig. 1b). Therefore, we confirmed that ITGAV was successfully overexpressed in dermal fibroblasts of the Tg mice.

Then, we compared skin phenotype of ITGAV Tg mice with that of WT mice. The macroscopic appearance showed no obvious difference between these mice. On the other hand, the histopathological findings of the skin revealed dermal thickness and Masson's trichrome staining were decreased in Tg mice compared with WT mice (Fig. 1c); The decrease in the dermal thickness was statistically significant ($p < 0.05$, Fig. 1d). Taken together, these results suggest that Tg mice showed thinned dermis accompanied by decreased collagen expression.

3.2. The expression of ECM-related molecules was altered in ITGAV Tg mice

The amount of ECM is one of the factors controlling dermal thickness. To clarify the mechanism underlying the reduced dermal thickness in Tg mice, the expression of ECM-related molecules was determined by immunoblotting. As expected, protein expression of ITGAV in the skin was significantly increased in Tg mice compared to WT mice (Fig. 2a, b). The expression of COL1A2 and α1(III) collagen (COL3A1) was reduced in Tg mice, while the level of α1(I) collagen (COL1A1) was not changed (Fig. 2a, b): The ratio of the expression of COL1A1/COL1A2 was slightly increased in Tg mice skin, but not statistically significant (Fig. 2c). On the other hand, integrin β3 expression was reduced by the ITGAV overexpression, while levels of integrin β1, β5, β6, or β8 was not affected (Fig. 2a, b). In addition, CTGF expression was down-regulated, while MMP-1 expression was up-regulated in Tg mice.

Consistently, mRNA levels of ITGAV or MMP-1 in Tg mice skin were also significantly up-regulated, and those of COL1A2, COL3A1, integrin β3 or CTGF was down-regulated in comparison to WT mice (Fig. 3). Considering that CTGF is known to induce tissue fibrosis while MMPs had negative effects on the amount of ECM, our results suggest that the down-regulation of CTGF, COL1A2 and COL3A1 as well as the up-regulation of MMP-1 at the mRNA levels contribute to the decreased dermal thickness in Tg mice.

3.3. In vitro experiments determining the expression of ECM-related molecules using cultured mice dermal fibroblasts

Next, to confirm in vivo results, dermal fibroblasts were cultured from the skin of WT and Tg mice. Immunoprecipitation analysis showed fibroblasts derived from Tg mice skin overexpressed ITGAV on the cell surface (Fig. 4a), but WT mice fibroblasts did not. Consistent with in vivo results, the up-regulation of ITGAV or MMP-1 and the down-regulation of COL1A2, COL3A1, integrin β3 or CTGF were also found in Tg mice fibroblasts at the protein and mRNA levels (Fig. 4b and c, respectively). The ratio of the expression of COL1A1/COL1A2 was slightly increased in Tg mice fibroblasts, but not statistically significant (Fig. 4d). To note, cell number of cultured Tg mice fibroblasts were decreased compared to fibroblasts of WT mice (Fig. 4e), and the decrease of cell proliferation was statistically significant (Fig. 4F), which may also contribute to the decreased dermal thickness of Tg mice. Consistently, Ki67-positive spindle fibroblast-like cells were decreased in Tg mice skin.

Similarly, cell surface expression of ITGAV was successfully increased by the transfection of ITGAV into NIH3T3 cells, compared to untransfected cells and empty vector-transfected cells (Fig. 5a). The significant difference was found only in the expression of ITGAV, integrin β3 and CTGF both at the protein levels (Fig. 5b, c) and at the mRNA levels (Fig. 6) between cells transfected with empty vector and ITGAV.

3.4. Decreased FAK phosphorylation mediates the down-regulation of CTGF and collagen in mice fibroblasts

We further determined the detailed molecular mechanisms that cause the alteration of ECM-related molecule expression in Tg mice skin, by focusing on integrin-associated signaling pathways. The relative levels of active TGF-β in the culture media (Fig. 7a) and phosphorylation state of Smad3 (Fig. 7b) in the Tg mice fibroblasts were not changed compared with those in WT fibroblasts. Thus, TGF-β signaling is less likely to be involved in the mechanism.

On the other hand, among the downstream signaling molecules of integrins such as FAK, paxillins and JNK, FAK phosphorylation was reduced in Tg mice fibroblasts in comparison to WT fibroblasts, although total FAK levels were not affected (Fig. 7b). We confirmed that integrin β3 siRNA inhibited FAK phosphorylation levels (Fig. 7c), and FAK inhibitor (R&D Systems, Minneapolis, MN) [14] decreased the expression of collagens and CTGF in mice fibroblasts NIH3T3 (Fig. 7d). Accordingly, reduced expression of collagen and CTGF in Tg mice skin may be explained by the decrease of integrin β3 and subsequent FAK phosphorylation.

4. Discussion

Integrins are thought to play various roles in each cell type. Many researches have been performed to clarify the role of ITGAV in each organ. For example, endothelial cell-specific conditional knock out mice did not show vascular phenotype [15]. Mice lacking ITGAV in the immune system showed loss of Th17 cells in the intestine and lymphoid tissues [16]. Furthermore, myofibroblasts-specific depletion of ITGAV using Pdgfrb-Cre system can prevent the lung and renal fibrosis [17]. On the other hand, as far as we have searched, skin phenotype of tissue-specific transgenic mice of ITGAV was not reported. In the present study, we performed in vivo and in vitro study using fibroblast-specific ITGAV transgenic mice, and expected skin fibrosis by increased collagen expression, as described in Introduction. However, the results indicated that overexpression of ITGAV resulted in decreased dermal thickness in mice skin. The decreased fibroblast proliferation, the down-regulation of COL1A2, COL3A1, integrin β3 or CTGF, as well as MMP-1 up-regulation may contribute to the skin change. This is the first study indicating the complex and paradoxical role of ITGAV in skin fibrosis.

Dermal thinning has been reported in SPARC-null mice and amino-terminally truncated isoform of p63 transgenic mice [18,19]: SPRAC is one of the matricellular proteins, and p63 is highly expressed in the skin and appears to be an early marker of keratinocyte differentiation. To note, fibroblast-specific knockout of integrin β1 resulted in the dermal thinning accompanied by less collagen expression [20]. Our hypothesis is that the balance between integrin α chain and β chain may positively or negatively control collagen expression and dermal thickness, and that the down-regulation of integrin β3 by the ITGAV overexpression as the negative feedback mechanism induced dermal thinning.

We proved that reduced expression of collagen and CTGF in Tg mice skin is due to the decrease of integrin β3 and FAK phosphorylation. Several previous researches already reported the effect of FAK on collagen expression [21,22]. Given that CTGF is one of the mitogenic cytokines of fibroblasts, reduced growth of dermal fibroblasts from Tg mice skin can be explained by the